12-2016

A Multi-Channel 3D-Printed Bioreactor for Evaluation of Growth and Production in the Microalga Dunaliella sp

Cristian A. Cox
University of Maine, cristian.cox@maine.edu

A MULTI-CHANNEL 3D-PRINTED BIOREACTOR FOR EVALUATION OF GROWTH AND PRODUCTION IN THE MICROALGA *Dunaliella sp*

By

Cristian Cox Seguel

B.S. Universidad Nacional Andres Bello, 1997

A THESIS

Submitted in Partial Fulfillment of the

Requirements for the Degree of

Master of Science

(in Biological Engineering)

The Graduate School

The University of Maine

December 2016

Advisory Committee:

Dr. Paul Millard, Associate Professor of Chemical and Biological Engineering, Advisor.

Dr. Michael Mason, Associate Professor of Chemical and Biological Engineering.

Dr. Peter Van Walsum, Associate Professor of Chemical and Biological Engineering.

A MULTI-CHANNEL 3D-PRINTED BIOREACTOR FOR EVALUATION OF GROWTH AND PRODUCTION IN THE MICROALGA *Dunaliella sp*

By

Cristian Cox Seguel

Thesis Advisor: Dr. Paul Millard

An Abstract of the Thesis Presented
in Partial Fulfillment of the Requirements for the
Degree of Master of Science
(in Biological Engineering)
December 2016

We explored the capabilities of additive manufacturing using a photo-cured jetted material 3D printer to manufacture a milli-microfluidic device with direct application in microalgae *Dunaliella sp* growth and intracellular compounds biosynthesis tests. A continuous microbioreactor for microalgae culture was CAD designed and successfully built in 1 hour and 49 minutes using black photopolymer cured by UV and a support material. The microreactor was made up of 2 parts including the bioreactor itself and a microchannel network for culture media fluids and microalgae. Both parts were assembled to form a single unit. Additional optical and auxiliar components were added. An external photodetection system platform helped to read light information coming from the bioreactor, related to microalgae growth and production of Carotenoids.

Several tests were carried out to check manufacturing quality, behavior of microalgae inside microreactor, quality of light based data coming from meauring system and comparison of microalgae culture operation using (flasks) and microbioreactor.

Growth of microalgae inside the microreactor was unsuccessful and several hypothesis may explain the lack of cell replication, from low CO_2 content to 3D photopolymer incompatibility with cell environment. Further improvements related to gas exchange, specially CO_2, microalgae retention system, high irradiance for light stressing tests and material biocompatibility need to be addressed in future works. From a mechanical point of view it was demonstrated the 3D fabricated microreactor it is possible and that it has promising advantages compared to other microfabrication processes that involve complexity in the design, longer manufacturing time, more expensive and sophisticated manufacturing techniques as well as specialized operators and designers.

ACKNOWLEDGEMENTS

I would like to thank my advisor Dr. Paul Millard for working under his guidance and allow me to participate in his wonderful laboratory, as well as for his patience to work with me the last year from overseas.

I would also like to thank my other committee members Dr. Michael Mason and Dr. Peter van Walsum for their technical ideas and constant support.

Inspirational supports from Dr. Peter Willis, JPL-NASA and Dr. Rose Mary Smith are very much apreciated.

I want to thank all of my classmates and colleagues who helped me at University of Maine and at the Center for Cooperative Aquaculture Research in Franklin. Many thanks to Dr. Nicholas Brown and CCAR director Steve Eddy. I would like to acknowledge instruments and laboratory space help from Dr.William Wolters and Dr.Gary Burr from USDA in Franklin. Many thanks to Wilson Adams for his great help in 3D printing manufacturing process and Dr.Gary Wikfors from NOAA, for microalgae supply.

Support, help and advice from Dr. Susan Brawley, Luz Kogson and Sarah Redmond are highly apreciated. I send my thanks to my friend, the late Susanna Simpson for helping me in passing the cruel winter of 2015 with humor and good stories.

Lastly, I would like to thank my family. My parents, Herbert Cox and Silvia Seguel for supporting my studies and projects, and my sons: Diego, Jose and Francisco for letting me share and enjoy with them new ideas in science.

TABLE OF CONTENTS

LIST OF TABLES

LIST OF FIGURES

CHAPTER 1

INTRODUCTION

1.1. Background and problem definition.

Biotechnological methodologies and instruments have been affected positively by the advantages of microelectronics and microfabrication techniques in general. Complex process automation and miniaturization of different types of sensors can be integrated in spaces that in the past was impossible to achieve.

Automatic control also has been applied to areas such as clinical microbiology, where one of the major hurdles is the manual processing of specimens. In comparison to chemical specimens, microbiological specimens are much more complex [30]. Application of automation in clinical microbiology, for example automated inoculation of samples, has been shown to be superior to manual inoculation with regard to pathogen recovery [31]. Automation enables a higher degree of standardization, which may be beneficial not only in terms of cost-effectiveness, but also in terms of gaining diagnostic quality [32].

In biotechnology laboratories tasks such as the screening of new bioactive compounds produced by genetically modified microorganisms, or determining optimal microbial strain growth parameters are typically carried out using tools such as test tubes, shake flasks and bench bioreactors. These are time-consuming and labor-intensive methods.

Currently, microtiter plates manipulated by robotic systems are being used as a front line tool in the biotechnology industry, sometimes employing integrated sensors. These microtiter plates can accommodate working culture volumes ranging from 0.1 to 3 mL. Temperature is easily controlled in microtiter plates but implementation of online pH and DO (dissolved oxygen) measurement in microtiter plates using optical methods has been partially successful. Restrictions imposed by working with certain microbial species at low pH, for example with yeasts at pH 5 driving optical sensors out of their preferred measurement range [1].

It is important to remark that most of present devices mentioned before, for example, microtiter plates used as tools for cell culture, are the type of batch culture.

There is a real need for high throughput devices that can handle continuous culture at small scale, since a continuous culture is an important tool to determine the response of microorganisms to their environment and to produce the desired products under optimal environmental conditions.

A bioreactor is an apparatus used to carry out specific bioprocesses, and examples may include fermenters or enzyme reactors [3].

Microbioreactors may resemble conventional bioreactors but their design requires re-thinking, since the behavior of materials, fluids for example, become dominated by surface tension, fluidic resistance and capillary forces at micrometer to millimeter length scale. Heat transfer phenomena in micro scale applications, may render stabilization of temperature challenging.

Microbioreactors can support low cost high throughput biochemical tests, in contrast to their macroscale counterparts, and they are beginning to find a wide range of applications in various fields such as drug discovery, high throughput bioprocessing, single cell analysis, stem cell research, genetic analysis among others [2].

Restrictions related to space, power, weight and material safety in spacecrafts make microbioreactors suitable tools to run continuous cell cultivation and different types of research essays in this type of environment [10].

Applications in bioprocess operations such as fermentation, where high value products like antibiotics, enzymes, vaccines and therapeutic proteins are produced in large scale would get a direct benefit in the starting phase of these processes where identification of best inoculum or best production conditions could be obtained by multiple, simultaneous parallel tests in a microreactor.

Betts *et al.* [12] concluded that most of the challenges to overcome in the development of microreactor systems is the variability of the tasks having to be performed and the difficulty of a single system to be able to satisfy all requirements. For example, in a growth medium development a need for parallelism is a priority in the device design whereas detailed strain characterization would require high degree of instrumentation for each bioreactor.

Development of precision micro-to milli-scale fluidic devices that are rapidly configurable and scalable is an area of much current interest [27] which is applicable to microreactors.

Fluidic devices, depending on their dimensions can be classified as nano (1–100 nm), micro (100 nm to 1 mm) or millifluidics (1–10 mm) [26].

If we want to be rigorous in the definition, this work deals with a device built using dimension scales in the very limit of micro to milli fluidics. Even though this device is in this intermedial area, we will present the theoretical background focused to fluid behaviour and properties in the microfluidic area.

According to Pasirayi *et al*. [2] Microfluidics bioreactors are fabricated using at least one of the following microfabrication techniques:

1.1.1 Photolitography

Photolithography allows high precision and reproducibility but requires a clean rooms and high capital infrastructure and high initial capital investment.

1.1.2 Soft Lithography

Soft lithography is based in the use of soft elastomers such as PDMS (Polydimethylsiloxane). This technique requires a template that will create the microfluidics patterns when PDMS is added and cured on the surface of this structure. This template may be created using photolithography or other technique that allow the creation of patterns in solid substances, the surface topography of which can be transferred to PDMS with spatial resolution in the micrometer to nanometer range [4]. As mentioned earlier, if photolithography is used for template production, the use or acquisition of specialized and costly equipment needs to be considered.

1.1.3 Hot Embossing

Hot Embossing involves the application of heat and pressure over a polymer substrate. A master mold, created in a complete separated process, is used to imprint features such as microfluidic channels into this surface. Specialized equipment is required for the application of the correct temperature and pressure . The microstructures created with this technique have high fidelity and aspect ratio in the nano and micro scale ranges. Materials like PMMA and polycarbonates can be used as polymer substrate [5].

1.1.4 Micro-Injection Molding

Micro-Injection Molding uses polymer material melted to liquid state that is injected into a mold.

This process is executed inside the injection molding machine where the polymer hardens after a cooling period and can be removed from the mold.

The high cost of mold fabrication is one of the drawbacks of this technique, but it permits the replication of thousands of microstructures or devices (composed or not composed) at low cost [6].

1.1.5 Direct Milling

Direct milling uses hard materials like PMMA, polycarbonates or some metals as substrates. It is a mechanical process that uses computer numerical control (CNC) to move and control the position of the milling device. There are drawbacks related to tension and stress in the material but at the same time the material is not exposed to degrading

factors such as heat, different type of radiation and chemicals used in other type of microfabrication processes, for example, in Photolithography.

There is a search for simpler and less cost- or time-consuming methods and techniques for the manufacturing of microfluidics devices.

Concidering new manufacturing methods, that until recently were not available, could now be used to design and manufacture microfluidic bioreactor systems on-site in a biological-biotech laboratory, rather than depending on an external manufacturing facility or common micro fabrication infrastructure and highly specialized equipment.

Additive manufacturing or three-dimensional printing (3D printing) technology is opening new possibilities in microdevice manufacturing.

In the past 3D printing has been used primarily for basic prototyping but its use for finished devices is increasing according to new technical advances in micro optical devices, optoelectonics and the reduction of material-equipment costs.

3D printing has been perceived as a technique with limited resolution, and not very useful in microfluidics fabrication, but the development, for example of Digital Micro Mirror Devices, has permitted resolution in the range of 50 μm in new affordable 3D printers [7].

The need for a rapid, reliable, simple and less expensive manufacturing method for a parallel microfluidic bioreactor, especially for users who are not involved in conventional microfabrication, is real. 3D printing could satisfy this need if

microbioreactor chambers, microchannels and additional components created with this technology meet the specifications required for cell culture and analysis.

Micro devices 3D drawings design files, easily downloaded in a laboratory computer may be available and for instance, a parallel-multi chamber microfluidics reactor, could be fabricated within hours and the micro device could be running biotests the same day in the laboratory. All this without using standard microfabrication techniques requiring sophisticated equipment and specialized personnel.

1.2. Project scope

This project is based on the thesis that a micro-milli fluidic bioreactor can be fabricated using simple, rapid, inexpensive and reliable additive manufacturing (3D printing), and that this device can be used to study microalgal growth and biosynthesis.

The fabricated microdevice should be capable of continuous culture and real time data acquisition, using the microalgae *Dunaliella sp* as a test microorganism.

Different tests will be carried out to assess the fabricated device respect to limits of design and possibilities as a real microorganism growing tool.

Bioprocess parameters like growing rate and carotenoid production yield under stressing and normal environments may be evaluated using this microdevice.

CHAPTER 2

THEORETICAL FOUNDATIONS

2.1. Overview of Micro-Milli fluidics bioreactors

Novel microbial cell cultivation technologies can enable high throughput screening and tests of new bioactive compounds, selection of useful strains for industrial bioprocess optimization and new methods for accelerating research in microbial physiology.

At present, microtiter plates represent one of the standardized tools in robot-assisted high throughput screening with microbial cells. Multiwell plates of up to 1536 wells are readily available and methods to control and monitor temperature, dissolved gases, pH, and mixing, for example, have been developed. The development and integration of new sensors and control capabilities into micro-bioreactors is the current challenge.

Culture of microorganisms in microplates is performed in a batch mode and so this technique presents a limitation for simulation of a continuous macro-culture.

2.2. Bioreactors and Microbioreactors

Bioreactors are devices in which biological processes, such as cell expansion, differentiation, or tissue formation on 3D scaffolds, can proceed under tightly controlled environmental conditions, involving gas exchange, nutrients, and metabolites, and application of molecular and physical regulatory factors [15]. Bioreactors may be

dedicated to mass production or they may be used to identify optimal physical/chemical parameters for the production of a specific product, such as a bioactive compound, or the most suitable microorganism for mass production. This process of identification can be carried out in small scale reactors where initial cost, labor, time and parameter control can be optimized easily.

At present, traditional scale up from a small volume test bioreactor to a larger volume production is highly empirical and is applicable only if there is no change in the controlling regime during scale up, particularly if the system is only reaction or transport controlled [33].

The main elements in the majority of liquid medium bioreactors are: culture chamber, systems for agitation, gas exchange and pumping, culture medium, waste reservoir, sensors and a control system. Batch, semi-batch fed and continuously fed bioreactors are the most common. Batch systems provide a single dose of nutrients in the medium for cell growth. In semi-batch fed, cells are allowed to grow for a period of time until the early stationary phase, at this point a fraction of the culture is harvested and the reactor is replenished with fresh medium. In continuously fed bioreactors, culture media is added at constant rate, resulting in a constant harvest of cells at the outlet of the reactor.

Bench scale bioreactors are important tools for cell cultivation for process optimization because it is possible to obtain rich sets of culture data by allowing a greater number of parameters to be tested and making use of sophisticated measurement and

control instrumentation. These devices still have limitations in terms of simple sterilization, assembly, cleaning, sensor calibration, and the number of parallel experiments that can be run, due to relatively large volume of these reactors [11].

An ideal microbioreactor would resemble a conventional bioreactor, but the fluidic system would be on the <100 μm length scale, entering into what is considered the microfluidic regime.

As the length scale of the microbioreactor decreases, the surface to volume ratio increases. As a consequence, fluidic dynamics are dominated by surface tension, fluidic resistance and capillary forces. Diffusive mixing becomes more important than turbulence, convective mixing, and gravitational forces [34].

The microbioreactor may combine the parallelism obtained with a microplate, with the improved capabilities of sensing and control for each culture chamber. It may also have the potential for use in continuous culture, rather than conventional batch mode, promoting rapid, cost effective comparison of growth/production conditions. It follows that design aspects such as material compatibility, mechanical forces, dissolved oxygen, pH, pCO_2, temperature, fluidic paths, a range of physicochemical factors, and both sensing and control elements, must be addressed to provide the cells or organisms with the optimum environment for growth and/or production.

The majority of research in microbioreactors has focused on their application in: microbial bioprocessing, stem cells, single cells, drug development and cytotoxicity [2].

2.2.1. Microfluidic devices

Microfluidics involves fluid flows over the <10 µm length scale. Precise control and manipulation of liquid or gases, commonly with femtoliter to microliter precision are performed through miniaturized conduits with different geometries and practical function [23].

In theory, microfluidic devices, among them, new types of microreactors could be built with advantages such as low power consumption, portability, small volume of reagents and samples, besides the advantages of working at similar length and time scales of cells, where short distances results in the reduced transport times of mass and heat which is ideal for local transport of growth factors secreted by growing cells in the cell's microenvironment [2].

Inside a microfluidic microreactor the fluid flow is laminar, which is ideal for analysis as cells can be exposed to controlled chemical gradients and their biochemical and morphological responses studied in vitro [24].

Length scales of structures inside a microfluidic microbioreactor would have similar dimensions of eukaryotic and prokaryotic cells, for example, allowing diffusion of oxygen and carbon dioxide in a manner similar to that in tissues [25] .

Fluidic, mechanical, electronic and optical systems can be integrated into a single, multifunctional microreactor platform. As mentioned earlier, there are four main microfabrication processes for microfluidic-millifluidic microreactors, these are: soft lithography, hot embossing, micro-injection molding and direct milling. At present, none

of these methods is easily accessible to non-specialized personnel outside of the microfabrication field, mainly because all of these methods require expensive fabrication equipment and facilities, in addition to highly skilled technical personnel.

Soft lithography, based on polydimethylsiloxane (PDMS,) is the most frequently used technique for microfluidic systems but requires master molds that are typically made by photolithographic, micromilling or e-beam lithographic techniques.

In this work we explore the possibilities and limitations of building a milli-microfluidic microreactor platform for microalgal growth and biosynthesis of biocompounds, using as a test microorganism the green microalga *Dunaliella.sp* and a manufacturing method based in additive manufacturing technique, commonly referred as 3-dimensional printing (3D printing) .

2.3. Additive Manufacturing

Additive manufacturing (AM) is a technique for creating 3D objects consisting of adding layer upon layer of a material, such as special types of organic polymers in liquid state, mixed with photocuring agents, fused polymers or metal powders. One way to classify additive manufacturing technologies is by the raw material used to create the layers.

At present there are four types of raw material that are commonly used:

(1) liquid polymer, (2) discrete particle, (3) molten material, (4) solid sheet.

2.3.1 Liquid polymer

One of the types of liquid polymers used today are liquid photopolymers, which are deposited in layers and the curing process of these layers is activated by a source of energy, for example a laser or by a high resolution display based on a digital micromirror device (DMD).

2.3.2 Discrete particle (DP) systems

Based on the deposition of a fine powder layer that after the application of energy (e.g. laser) or a chemical treatment to bind the particles together, a solid layer is created.

2.3.3 Molten material systems (MMS)

Raise the temperature to levels at which the structural materials reach their melting point and flow through a delivery system to create a layer of material. A well known system of this type is fused deposition modeling (FDM), in which the material to be fused is extruded through a nozzle that delivers it in a controlled manner.

2.3.4 Solid sheet systems (SSS)

Based on the addition of layers (for example paper coming from a continuous roll) that is cut in patterns and the layers are bonded with a heat-activated resin embedded in the paper.

Additive manufacturing comprises 7 process categories that are in accordance with ASTM/ISO standardization:

2.3.5 Vat Photopolymerization

Liquid photopolymer is cured by selective application of energy in a specific region.

2.3.6 Powder Bed Fusion

Material powder is selectively fused using a source of energy, for example a laser or electron beam.

2.3.7 Material Extrusion

A nozzle extrudes and delivers material in specific regions, creating structural patterns.

2.3.8 Material Jetting

Inkjet printing of material (e.g., photopolymer) through production of tiny droplets of liquid UV-curable photopolymer. Fine layers accumulate on the build tray to create a precise 3D model. Printers of this type may have the option to include additional materials with different characteristics (e.g., mechanical or color). A support material also may be required to avoid the collapse of structures and patterns when the design includes cavities or empty spaces inside the structure. This gel-type support material is typically removed with pressured water and discharged after the completion of the whole structure.

2.3.9 Binder Jetting

A roller is used to spread a layer of powder onto a build platform. The mechanical system ensures that the bed is filled with a layer of packed powder. A print head applies a liquid binder to create a cross section of the object on the powder. In this case the powder is the medium and would be the equivalent of a paper in a inkjet printer. The process is repeated and a new powder layer is applied with the correspondent dispensing of liquid binder on the specific areas for creating the structure. Support material is not required in this process.

2.3.10 Directed Energy Deposition

Delivery of energy and material at the same time through a single deposition device.

The use of additive manufacturing in bioengineering applications has been growing steadily in the past years because its inherent advantages, including the ability to make optimized and very complex customized parts that are useful in biological environments, such as dental prosthetics and tissue engineering.

3D printing has been applied in microfluidics, either as a tool for manufacturing PDMS templates, or fabrication of complete polymerized micro/millifluidics devices.

3D Reactionwares (refers to devices that combine both reactor and reagent, catalytic or architectural control of the reaction outcome). Chemical synthesis [8],

chambers, templates for PDMS LOC devices [7], micromixers, gradient generators, droplet extractors, and isotachophoresis devices, have been successfully built.[9]

Some of these later devices could be fabricated in 12-20 minutes with a material cost of 0.48-1.00 US$. Lee et al [11] have devised a new method for detection of pathogenic bacteria in food using a novel 3D-printed helical microchannel, and Au et al [16] have integrated 3D-printed automatic control devices to other microfluidic devices.

2.4 Dunaliella sp

The green microalga *Dunaliella sp* was chosen as a test organism to explore the advantages and limitations of a microfluidic bioreactor built using an additive manufacturing technique as a tool for exploring algal growth/biocompound production conditions. Growth rate and carotenoid production by *Dunaliella* species were parameters used to report algal activity in the microreactor. These data speak to material biocompatibility, fluidics design, sensing-detection and the capacity of the microreactor itself to act as an effective tool for studying microalgae.

Dunaliella sp is a biflagellated unicellular algae classified under Chlorophyceae, Volvocales and includes marine and fresh water species. *Dunaliella* cells are ovoid, spherical, pyriform, fusiform or ellipsoid with size varying from 5 to 25 µm in length and from 3 to 13 µm in width [47]. *Dunaliella sp* present one large chloroplast with single-centered starch surrounded by a pyrenoid, vacuoles, nucleus and nucleolus. A polysaccharide cell wall is absent and the microalga is enclosed by a thin elastic plasma membrane covered by a mucous surface coat [17]. This microalga has can tolerate

sudden changes in solute concentration as well as varied light irradiance (potentially a stress condition) and nutrient availability [18].

2.4.1 Salinity

Changes in the salinity of the extracellular environment cause changes in the volume of the cell, which are accomodated by the lack of a cell wall. *Dunaliella sp* responds to salt stress by massive accumulation of glycerol, enhanced elimination of Na^+ ions and accumulation of specific proteins [35] to compensate for changes in the osmotic pressure of its environment that could be lethal for other species of microalgae.

Dunaliella sp can adapt to extreme environments (stress environments) that range from salinities lower than seawater (0.1M NaCl or 0.5844 g/L) to saturated salt solutions (5M NaCl or 292.2 g/L) [37].

2.4.2 Light irradiance and Carotenoids

Damaging high light irradiance is compensated-for by synthesis of high intracellular concentrations of carotenoids [19]. Carotenoids constitute a class of terpenoid pigments that are derived from a 40-carbon polyene chain. This molecular structure gives carotenoids a distinctive molecular structure and associated chemical properties, including light-absorption that aids photosynthesis and facilitates life in the presence of oxygen. Hydrocarbon carotenoids are denoted as carotenes, but this group gives rise to a derivative group denoted as xanthophylls which contains oxygen in the form of hydroxyl moieties or/and oxygen acting as a bridge in epoxides [48].

Some examples of carotenes are: lycopene, beta-carotene, and alpha-carotene. Examples of xanthophylls are: Lutein, cantaxanthin, astaxanthin, violaxanthin, fucoxanthin, zeaxanthin, and neoxanthin.

Experiments using different levels of light irradiance to induce stress have been reported, and these resulted in varying levels of intracellular carotenoids. For example, Fazeli *et al* [21] used 50 µmol/m²s as normal irradiance and 150 µmol/m²s as the stressing irradiance, while Kleinegris *et al* [36] used 206 µmol/m²s as normal irradiance and 1672 µmol/m²s as stress irradiance.

When *Dunaliella salina* cells are light stressed, they produce higher levels of carotenoids. The green cells, the pigment of which is dominated by the chloroplast, begins to turn orange. The chloroplast shrinks, chloroplast membranes decrease in size, and carotenoid-containing lipid globules are formed. This color change was clearly evident by light microscopy with 1672 µmol/m²s as a stress irradiance [36].

Carotenoids autofluorescens in solution has been demonstrated [38]. Kleinegris *et al* [36] have obtained fluorescence in the range of 505–530 nm with exitation wavelengths of 450, 488 and 510 nm. This autofluorescens property could be used in some manner to measure intracellular production.

CHAPTER 3

METHODS

3.1. Microreactor conceptual design

Simplicity, applicability to continuous culture, physicochemical and biological requirements for the normal growth and stress of microalgae, nature of microalgal tests, materials costs and equipment availability were taken in consideration in the design of the microreactor for Dunaliella culture.

Figure 3.1 is a conceptual representation of the device.

Microalgae must be retained inside of the culture chamber when media is being injected into the chamber. A 1 μm pore mesh was therefore used to retain the microalgae.

The temperature of the chamber was to be controlled automatically by external resistive heating elements placed and covered by a flattened plastic ribbon that could be cut to the size of the microdevice and placed on the top of the reactor. This idea was ultimately rejected because the heat produced by LEDs (RGB led and UV led) was not negligible and these could serve as a heat source for reaching a culture temperature suitable for normal microalgaal growth.

Carbon dioxide (CO_2) and nutrients could be supplied along culture media directly through microchannels to the culture chamber.

A Red-Green-Blue color LED pointing to the culture chamber was the main source of light and played three different roles in the light system: (1) as light for normal growth conditions, (2) as a stressor for inducing physiological changes inside of the algae, and (3) as part of the analytical system for measuring turbidity (optical density, OD) or fluorescence.

A second source of light was a UVA LED, which was also directed into the culture chamber but from the opposite side from the RGB LED This UV light provided stress illumination for experiments involving light-mediated stress.

Turbidity measurements in each microchamber were based on light scattering, requiring the light from the RGB Led to be collimated prior to entry into the chamber, reducing undesired noise in detector photodiode positioned at a 90 degree angle with respect the RGB LED.

Since microlagae carotenoid fluorescence and light scattering are measured at 90 degrees with respect to blue and green light incident light, respectively, two possible detector locations were tested. One sensor was located at the bottom of the reactor via an aperture in the chamber sealed by a window consisting of a glass slide. Here, the photodetector was mounted on an external circuit board facing the bottom window. The second location was an optical fiber that exended directly to the microchamber through a specially made cavity and the fiber was coupled to an external photodetector.

The same window for the bottom photosensor can also be used for microscopy when direct observation of the culture is desired.

A microalgae agitation system, was designed to provide adequate exchange of nutrients and gases, good light exposure and removal of waste material. Its function depends on the hydrodynamic forces stemming from the flow of fresh media coming at the bottom outlet inside the chamber.

The microreactor structure consists of two parts that can be disassembled to accomodate changing the microalgae retention mesh or for cleaning procedures, allowing the reactor to be reused for different tests.

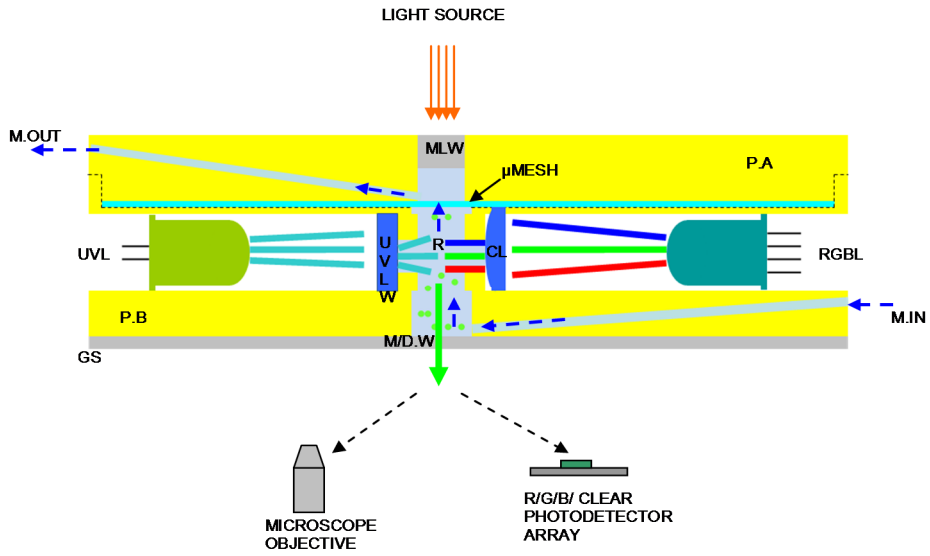

Figure 3.1 Microreactor conceptual design. Culture Medium oOutlet (M.OUT); Microscopy Light Window (MLW); 1 µm pore polymer mesh (µMESH); Photopolymer part A (P.A); Photopolymer part B(P.B); UV Led (UVL); Red Green Blue LED (RGBL); UV Light Window (UVLW); Reactor Chamber (R); Collimator Lens (CL); Culture Media Inlet (M.IN); Microscopy-Photodetector Window (M/D.W); Glass Slide (GS).

3.2. Device design and fabrication

3.2.1 Microreactor design

The device as mentioned before, was formed by two main parts, A and B (upper and lower parts, respectively), see Figures 3.3 and 3.4.

These parts were designed using the computer-aided design (CAD) software for Windows 8, Solid Edge ST6 (Siemens 2013.

CAD 3D design files were transformed from STL files into 3D modeling slices using Stratasys Objet Studio Software (Windows 8). 3D modeling slices include the information for support and building material. Using the same software the CAD designed parts were aligned and placed in an optimal position before continuing with the next building steps.

The design took into account cavities for fast and easy insertion and removal of RGB and UV LEDs. RGB LEDs consisted of 3 semiconductor color devices inside of a single LED with a 5 mm clear epoxy case and spectral outputs centered at 620, 515 and 480 nm (Ultra bright red, green and blue, respectively (LEDRGBE, Thorlabs Inc, Newton, New Jersey, USA). UV LEDs (Ultra Bright Deep Violet Led, LED370E, Thorlabs Inc, Newton, New Jersey, USA) also had a 5 mm clear epoxy case and the spectral output peak is at 375 nm. We planned to use a collimator lens to increase the efficiency of the microalgae cell density detector.

Collimating lenses are optical lenses that help to make parallel the light (coming from the RGB LED in this case) that enters the meter setup, in our case, the microchamber and the photodetector at 90 degrees. With this type of lens is possible to control field of view, collection efficiency, spatial resolution, configure illumination and collection angles for sampling. RGB LED light was collimated using a 5.2 mm diameter molded plastic aspheric lens (Thorlabs Inc, Newton, New Jersey, USA) to minimize noise and maximize the the microalgae-scattered light signal that is received by the photosensor at the bottom of the microchamber window (at 90 degrees from the RGB LED collimated beam). The effective focal length of the lens for light collimation optimization is given by the equation:

$$f = (\Phi/2) / \tan(\theta/2)$$

Where f is the focal length of the lens (mm), Φ is the collimated light beam diameter (mm) and θ is the RGB LED divergence angle. In this case f = 9.85 mm, Φ = 3.46 mm, θ =19.9 °. Figure 3.2 shows an ideal representation with a single source of light and does not consider that the three semiconductor color dies inside the RGB LEDs had some degree of eccentricity relative to the longitudinal axis.

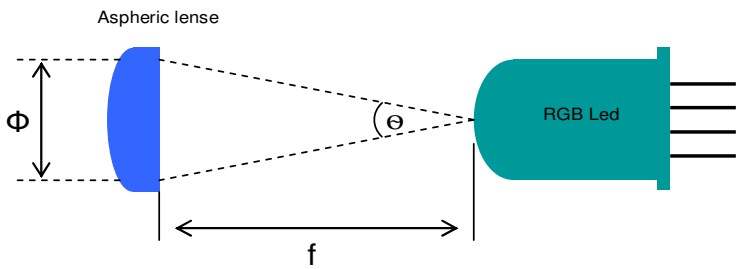

Figure 3.2 RGB Led Light collimation using an aspheric lens.

The reactor design includes a rectangular cavity, see figure 3.6, between the microreactor chamber and the RGB LED, for the collimator lens installation.

The collimator lens was glued to the lateral chamber window to avoid leakage of liquid growth medium. Sealing was accomplished using UV-curable clear optical adhesive (NOA60, Norland Products, Cranbury, NJ, USA)

After the lens was sealed to the lateral window, a photopolymer cover was used to cover this cavity and to avoid light escape and interference with the adjacent scattered light photodetector, see Figure 3.6.

The UV LED also required a lateral window in the microchamber to transmit light into the medium and the microalgae. This window was created by injecting UV curable clear optical adhesive (NOA60, Norland Products, Cranbury, NJ, USA) through one small slot between the UV LED and the microreactor lateral window. Leakage of adhesive into the microchamber itself before the adhesive was completely cured was prevented using an external UV light source.

Parts A and B are assembled after placing a 1.0 micron mesh (Nylon, Nitex) screen cloth between them. Microreactor outputs R1, R2 and R3, see figure 3.3, were covered by the mesh, filtering the culture media entering into the chamber containing the microalgae. Each microreactor output, and Nylon mesh, was sealed with clear silicone sealant (Loctite® Clear Silicone waterproof sealant), taking care to avoid obstruction of the outputs, but isolating each reactor output to avoid media cross contamination.

Part A, filtering mesh and Part B were assembled in one unit and screws were used to affix the parts to one another.

At the bottom of the reactor, a glass slide was glued to the polymer flat surface using Clear Silicone to prevent media leakage, and at the same time making sure that the bottom microreactor window for microscopy and photodetection was not obstructed, see figure 3.6

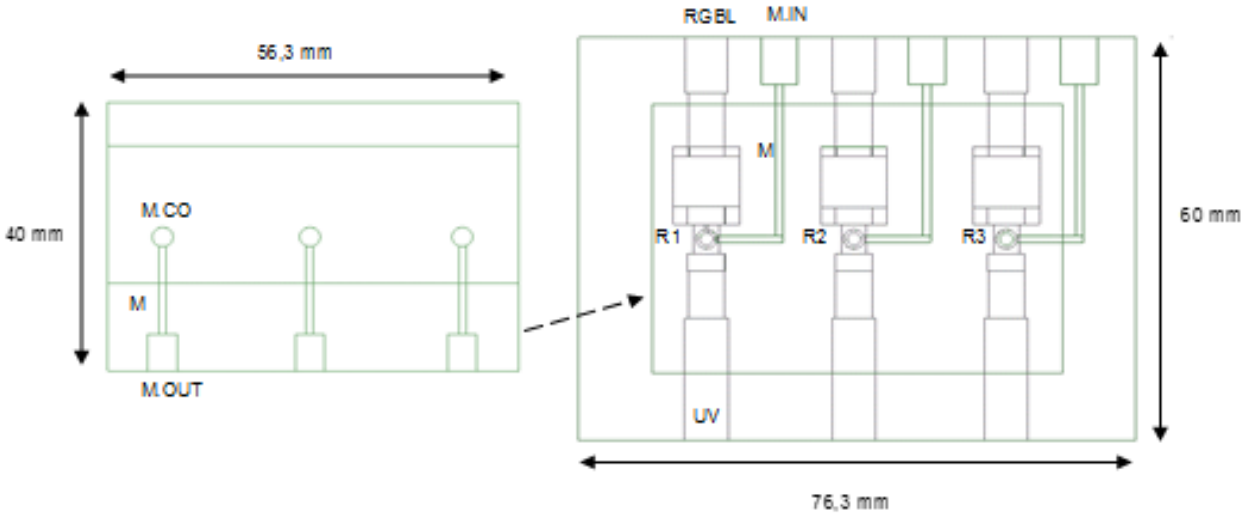

Figure 3.3 Three chambered microreactor array CAD design, top view. Photopolymers: parts A and B (left and right, respectively). Part A is mounted on top of part B, placing a 1 micron mesh between both flat parts. (M.CO) culture media collector; microchannel (M); Culture Media outlet (M.OUT); UV Led insertion (UV); Red Green Blue Led insertion (RGBL); Culture Media Inlet (M.IN); Reactor chambers 1,2 and 3 respectively (R1-R2-R3).

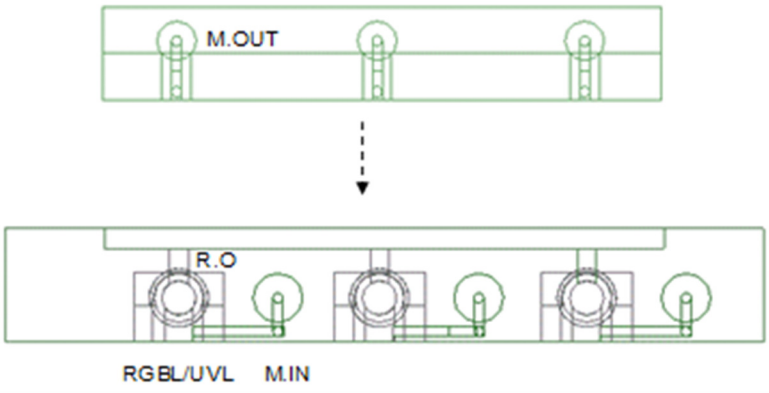

Figure 3.4 Microreactor array (3 chambers) lateral views. Photopolymer part A (top) and photopolymer part B (bottom). Part A is mounted on top of part B. Culture Media inlet (M.IN); Culture Media outlet (M.OUT); UV Led insertion (UVL); Red Green Blue Led insertion (RGBL).

The culture media is injected into the media inlet and flows through a 1 mm diameter microchannel to the bottom of the microchamber (see Figure 3.5) producing microalgae agitation and mixing of media from the bottom to the top for adequate nutrient distribution, gas transfer and maintenance of microalgae in suspension. Media and microalgae, lifted from microchamber bottom, are filtered by the mesh placed immediately before the media collector area, which leads to the media outlet through a 1 mm microchannel.

The culture media collector area (MCO) (see figures 3.3 and 3.5) is sealed from the external environment using a 3.0 mm diameter, 4 mm long clear light pipe as a plug (see figure 3.7 (MLW)). This plug was sealed to the photopolymer material using UV curable clear optical adhesive (NOA60, Norland Products, Cranbury, NJ, USA).

The transparency of the plug on the top of the media collector area helps as a light source entrance to permit observation using an inverted microscope.

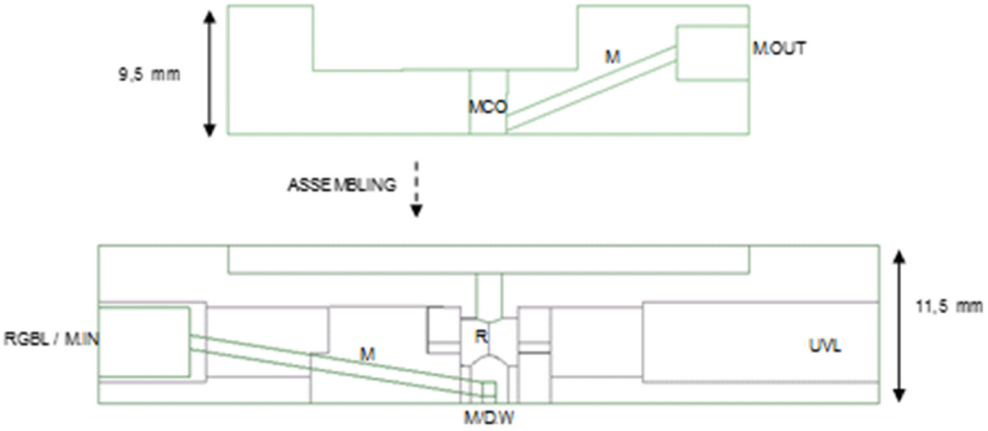

Figure 3.5 Microreactor array lateral view (1 chamber view only). Photopolymers: parts A and B (top and bottom respectively). Culture Media outlet (M.OUT); UV Led insertion (UVL); Red Green Blue Led insertion (RGBL);Reactor Chamber (R); Culture Media Inlet (M.IN); Microscopy-Photodetector Window (M/D.W); culture media collector (M.CO); microchannel (M).

After fabrication, culture media inlets and outlets (see Figure 3.6; M.IN and M.OUT) were threaded using a tapping tool for the installation of tubing adapters (thread to hose barb adapter, 1/8" NPT(M) to 1/16" ID , Cole Parmer Instrument Company LLC).

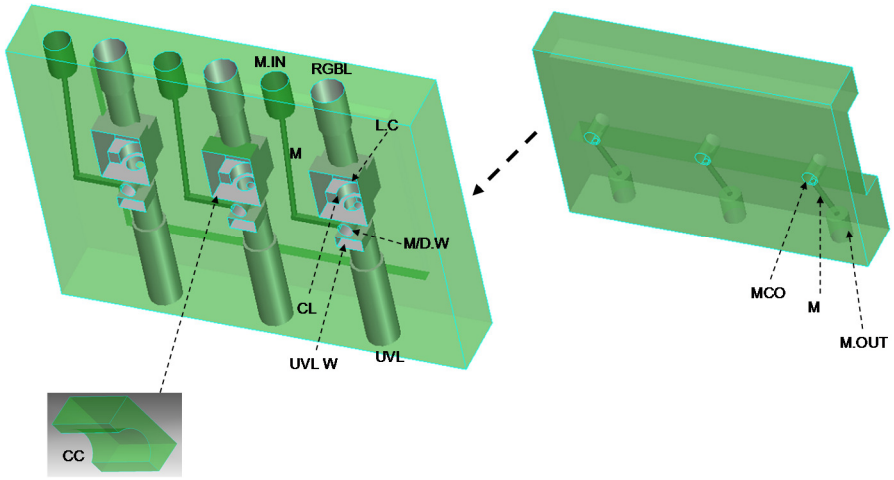

Figure 3.6 Microreactor array 3 dimentional design bottom view. Photopolymer parts B and A (left and right respectively). Culture Media outlet (M.OUT); UV Led insertion (UVL); Red Green Blue Led insertion (RGBL); Reactor Chamber (R); Culture Media Inlet (M.IN); Microscopy-Photodetector Window (M/D.W); culture media collector (M.CO); microchannel (M); UV light window (UVLW); Collimator lens placed at lateral chamber window (CL); Lens cavity (L.C); Cavity Cover for light leaking (CC).

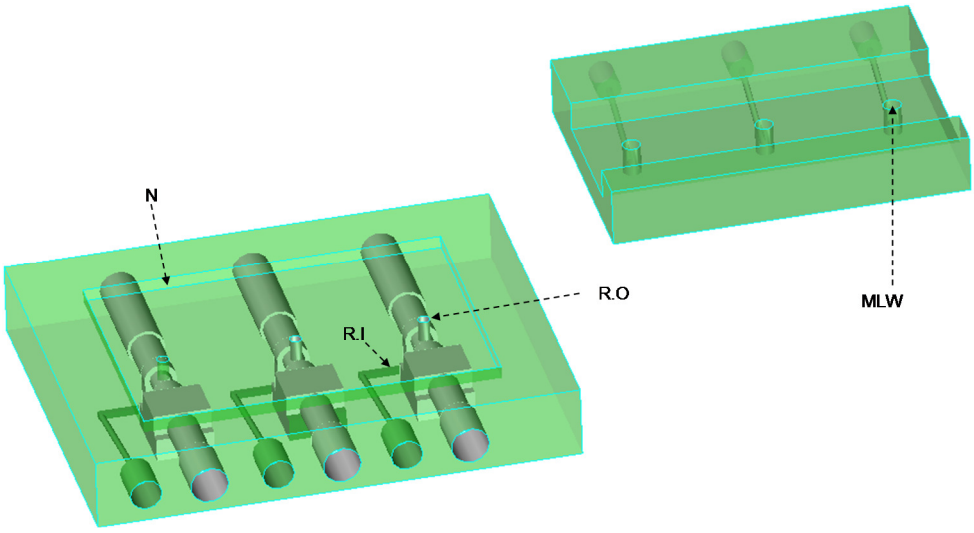

Figure 3.7 Microreactor array 3-dimensional design top view. Photopolymers: parts B and A (left and right respectively). Notch for placing part A on top (N) (1 micron mesh between parts A and B); Reactor inlet (R.I); Reactor outlet (R.O); Microscopy Light window (MLW).

3.2.2 Microreactor fabrication

A 3D printer Objet30 Pro (Stratasys, Polyjet Technology USA-Israel) (20.000 US$) was used for the microreactor fabrication, see figure 3.8. The printer can be used for high-end rapid prototyping with a build resolution: X-axis: 600 dpi; Y-axis: 600 dpi; Z-axis: 900 dpi and accuracy of 0.1 mm. With 2 printing heads 3D structure layers are created by jetting tiny droplets of liquid UV-curable photopolymer and support material. A nontoxic support material (Stratasys, Polyjet Technology USA-Israel) gel-like photopolymer is also required for avoiding the collapse of structures and patterns. The support material is washed out using pressured water after the building process is complete.

The thickness of the printed layer is 28 µm with printing speeds of 120 cm^3/hr for opaque material and 60 cm^3/hr for clear material.

The printer is 82.5 × 62 × 59 cm in size and weighs 106 kg. The tray (where the 3D structure is built) is 300 × 200 × 150 mm.

Figure 3.8. 3D printer Objet30

Even though three identical reaction chambers were planned for the complete reactor, as proof-of-concept only one chamber was manufactured and prototyped (see Figures 3.9 and 3.10) before expanding and manufacturing a 3-chamber device.

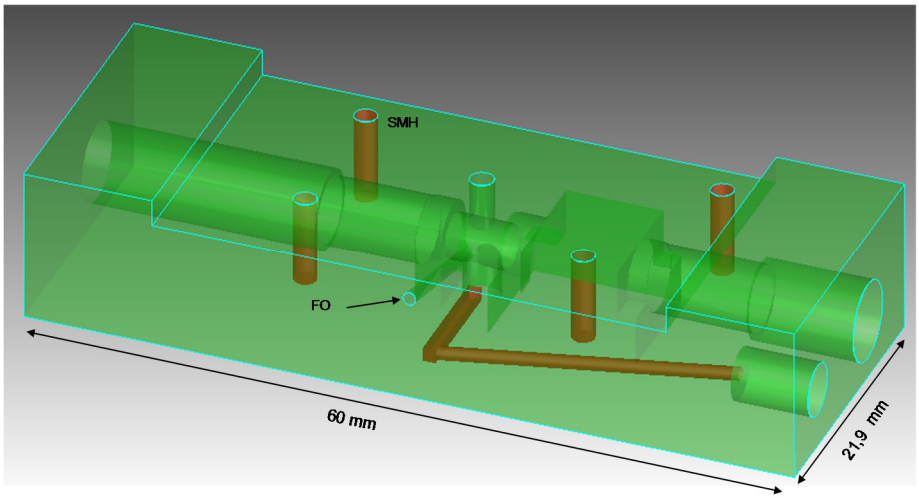

Figure 3.9 Single microreactor, (part B). Screw mounting hole (SMH); Fiber optics insertion (FO).

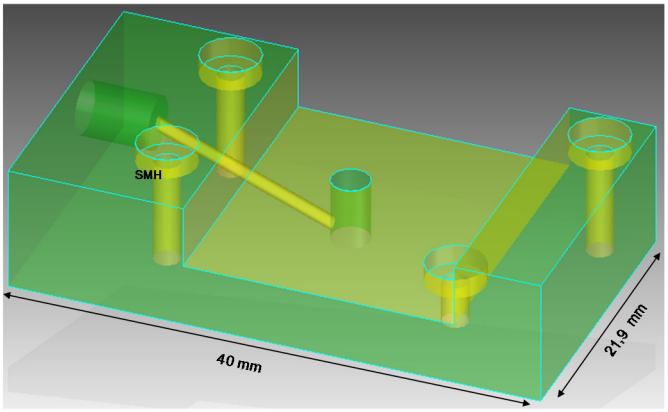

Figure 3.10 Single microreactor (part A). Screw mounting hole (SMH).

This one chamber prototype incorporated a fiber optic inserted at 90 degrees to the horizontal chamber axis (source of light axis) (see Figure 3.9.)

In this design the optical fiber should have reached the microculture chamber and direct scattered light to an external RGB clear photodetector array to act as a fluorescence and scattered light detector (for intracellular carotenoids and turbidity, respectively) as an alternative to the original design in which the same RGB clear photodetector array detector at the bottom of the chamber was used (see figure 3.6 (M/D.W). In this way it couldbe determined which detection method was perferred.

For the first and second prototype, the material used in device fabrication was Durus™ White, which is a proprietary material, the composition of which is based on a mixture of Isobornyl acrylate, acrylate oligomer, acrylic monomer and a photoinitiator, and ultimately mimics the physical properties of polypropylene (PP).

For one chamber prototype, 45 g of photopolymer material was used, with a cost of 0.9 US$/g and 17 g of support material with a cost of 0.4 US$/g.

For both prototypes (either Durus™ or Vero ™ material) the building time was 1 hour 49 minutes.

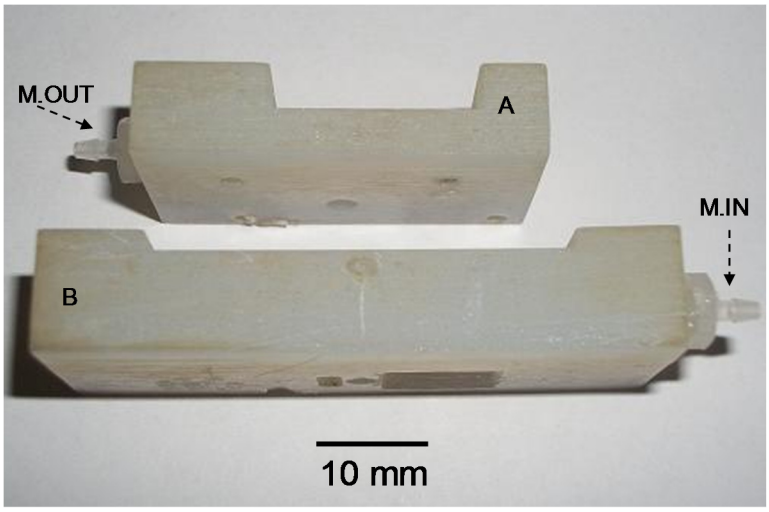

Figure 3.11 Reactor parts A and B prototypes. Photopolymer material Durus™ White. Culture Media Outlet (M.OUT); Culture Media Inlet (M.IN).

Support material that adhered to surfaces on the structure was washed out using water under pressure. This was accomplished on exposed surfaces or surfaces where mechanical force of the water treatment was sufficient to wash out this material.

After pressure washing the structures, the parts were placed in ultrasonic bath for 10 min at 80 C°. A subsequent pressure washing step was performed to rinse out any remaining debris.

In the case of internal structures, specially microchannels of 1 mm in diameter (see Figure 3.15 (M)) it was not possible to remove support material using the pressurized water procedure specially because the force of the water was not strong enough to penetrate and scrub the walls of these internal 1 mm microchannels. To clean these more effectively, the structure was warmed up to 80 C° in a water bath for 10 minutes and then a 1 mm rigid wire was inserted into the culture media inlet, reaching the microchannel elbow. This was sufficient to push the gel-like support material out through the reactor inlet (see Figure 3.7 (R.I).) To completely clear the channel, the same procedure was executed in the opposite direction, inserting the wire into the reactor inlet in the direction of the elbow, and again pushing material out through the culture media inlet. This procedure was carried out several times until the microchannel was completely cleared. After this cleaning procedure a syringe was used to inject water through the channel several times to remove any remaining debris.

The reactor was then dried and female threads were tapped into the polymer material for the insertion of male tubing adapters.

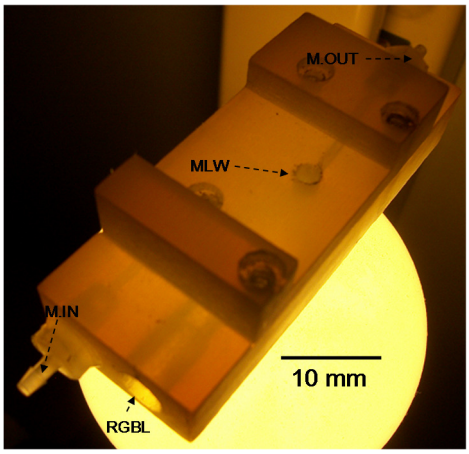

Figure 3.12 Preassembled part A and B showing internal features. Culture Media Outlet (M.OUT); Culture Media Inlet (M.IN); Red Green Blue Led insertion (RGBL); Microscopy Light Window (MLW).

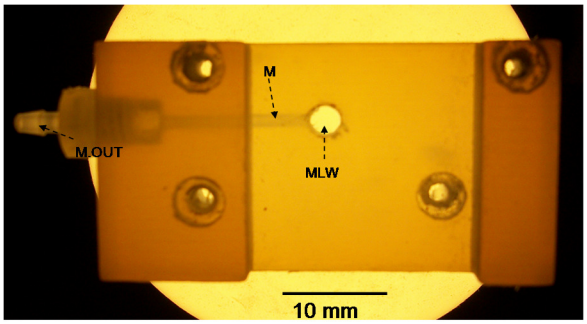

Figure 3.13 Part A internal features. Culture Media Outlet (M.OUT); Microscopy Light Window (MLW); Microchannel(M).

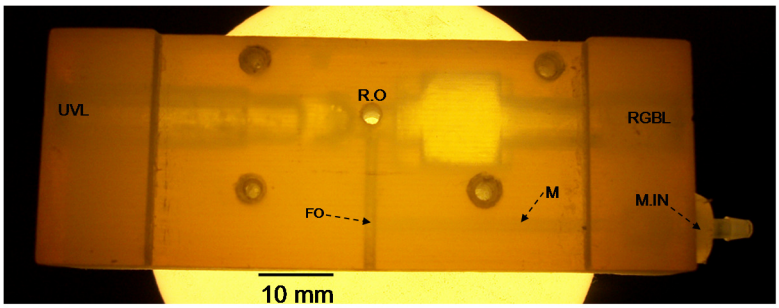

Figure 3.14 Part B, top view, internal features. Culture Media Inlet (M.IN); Microscopy Light Window(MLW); Microchannel(M); Reactor Outlet (R.O); UV Led insertion (UVL); Red Green Blue Led insertion (RGBL); Fiber optics insertion (FO).

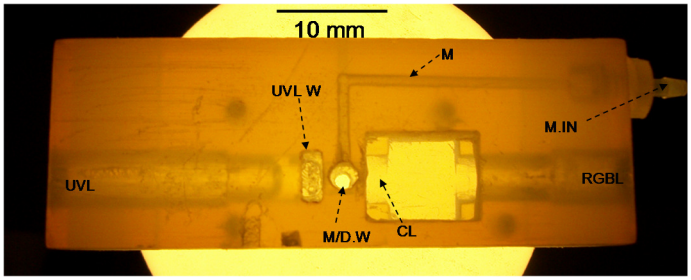

Figure 3.15 Part B, bottom view, internal features. (M.IN) Culture Media Inlet; (M) Microchannel; (UVL) UV Led insertion; (RGBL) Red Green Blue Led insertion; (M/D.W) Microscopy-Photodetector Window; (UVLW) UV light window; (CL) Collimator lens placed at lateral chamber window.

In the case of photopolymer material Durus™ White, when the RGB LED is active, light is transmitted through the whole assembled microreactor structure(see Figure 3.16.) This is a problem for light scattering and carotenoids fluorescence measurement, since the light detected at 90 degrees at the bottom of the microchamber through the Microscopy-Photodetector Window (M/D.W) should ideally only come from light scattered by cells suspended in the media.

This is also a potential problem for a multi-chamber design in which three micro culture chambers are built in the same structure, permitting three experiments employing different light intensities or photoperiods to be carried out. In this case the light intensity or a photoperiod sequence of one chamber could interfere with that of an adjacent chamber.

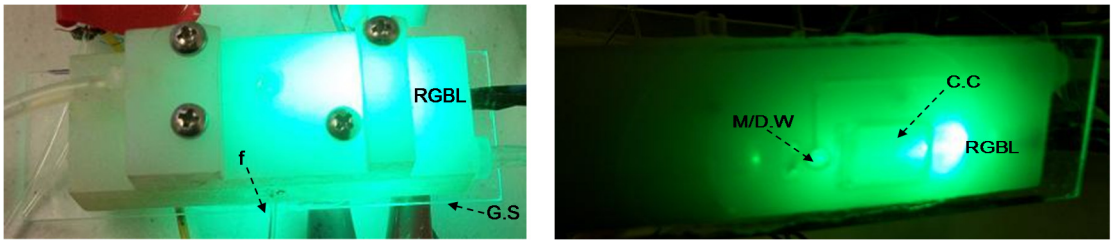

Figure 3.16 Part A and B assembled with a glass slide on the bottom. Top and bottom view (left and right, respectively) and internal features. Red Green Blue Led insertion (RGBL); Microscopy-Photodetector Window (M/D.W); Cavity Cover for light leaking (CC); Fiber optics (f); Glass slide (G.S).

To solve his problem a third prototype was built using a Vero™ Black material (see Figure 3.17), also a proprietary plastic (Stratasys, Polyjet Technology USA-Israel). This is an opaque material that mimics acrylonitrile butadiene styrene (ABS). The main constituents of this material are: acrylic monomer, isobornyl acrylate, phenol, 4,4'-(1-methylethylidene)bis-, polymer with (chloromethyl) oxirane, 2-propenoate, diphenyl-2,4,6-trimethylbenzoyl phosphine oxide, acrylic acid ester, m- and p-xylenes, propylene glycol monomethyl ether acetate, n-butyl acetate, carbon black, and ethylbenzene.

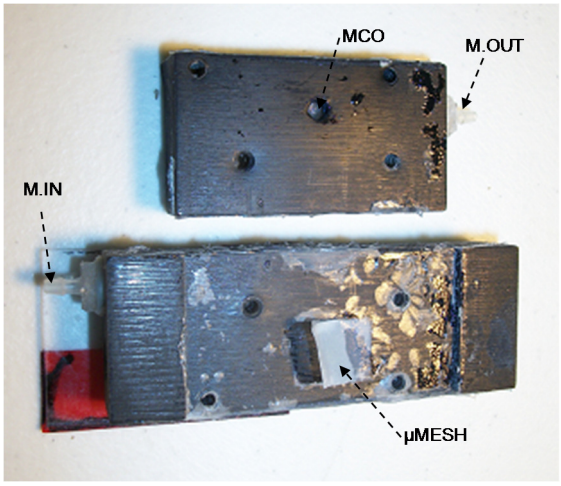

Figure 3.17 Third reactor prototype built using photopolymer Vero™ Black. Culture Media Inlet (M.IN); culture media collector (M.CO); Culture Media Outlet (M.OUT); 1.0 micron nylon (Nitex) mesh screen (µMESH). Microreactor mounted on glass slide.

3.2.3 Microreactor final assembly

In the third prototype printed using Vero™ Black (opaque material), any support material, particularly that left inside of the microchannels, was rinsed out using the same washing procedure used for Photopolymer material Durus™ White. After a final rinse, part A and B were dried using a pressurized air pistol.

The aspheric collimator lens was placed and cemented to the photopolymer material, at the same time sealing the reactor lateral window from media leakage (see Figure 3.18) using UV-curable clear optical adhesive (NOA60, Norland Products, Cranbury, NJ, USA), then a cover made specifically for this application was placed over the cavity to avoid additional light leakage. Using clear silicone (Loctite® Clear Silicone waterproof sealant), the glass slide was affixed to the flat bottom of the reactor, sealing all possible leaking points including the micro chamber bottom window.

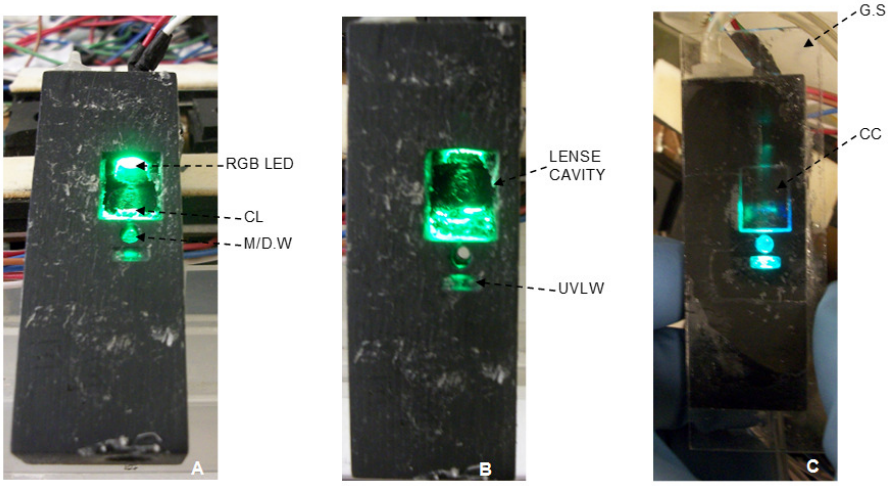

Figure 3.18 Microreactor bottom view. Third and final prototype showing RGB led, lens cavity and collimator lens system. Collimator lens (CL); Microscopy-Photodetector Window (M/D.W); UV Light Window (UVLW); Cavity Cover (CC); Glass slide (G.S).

After attachment of the cavity cover (see Figure 3.18 C), a small amount of light leakage through the cavity cover rim and part of the cavity cover itself,was detected. This problem was avoided by applying black tape to the light leakage area on the glass slide. The same modification was made with the UV light window.

A 10 mm x 7 mm 1.0 micron nylon mesh (Nitex) screen cloth rectangle was cut and placed on top of the reactor outlet hole, located immediately before the media collector in part A, so that the mesh layer separated part A and B, filtering the culture media and not permitting the microalgae to escape from the microchamber. Figure 3.17 shows the mesh and some remains of clear silicone (Loctite® Clear Silicone waterproof sealant) after the reactor assembly was opened to expose the components.

The mesh was glued and sealed to the surface using clear silicone (Loctite® Clear Silicone waterproof sealant), being careful not to obstruct the culture chamber outlet, but putting enough sealant to stop any lateral leaking between part A and B when they are put together. The reactor outlet (R.O) was covered by the mesh (see Figures 3.7 and 3.17) and this outlet needed to be aligned perfectly with the media collector (MCO) and Microscopy Light Window (MLW) (seefigure 3.19.) The mechanical design allowed this alignment to be performed as soon as part A and B were mounted correctly.

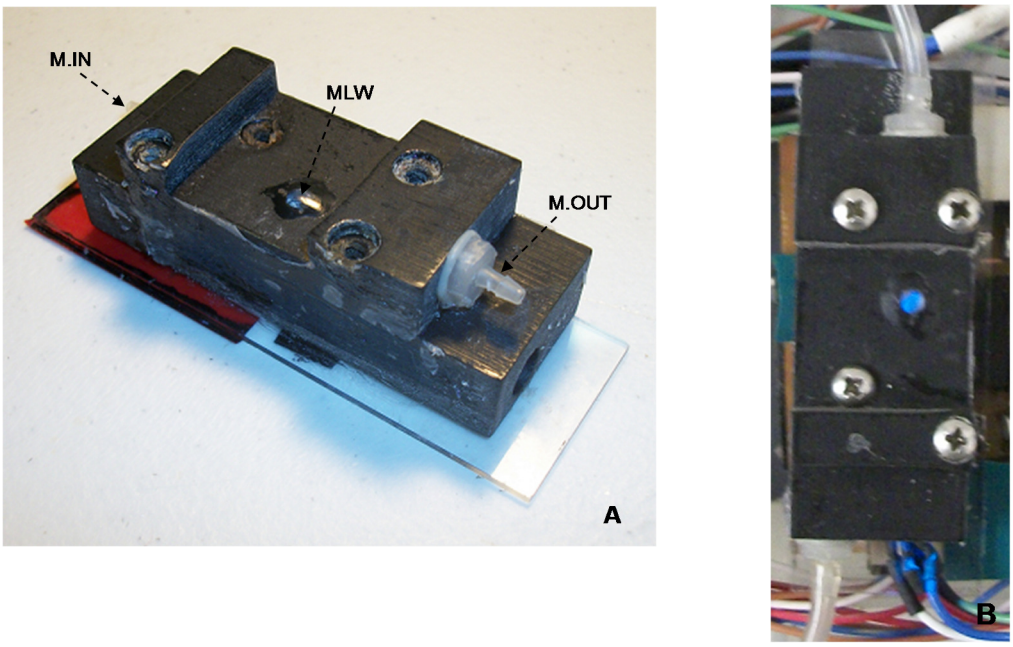

Figure 3.19 (A) Final assembled prototype. Culture Media Outlet (M.OUT); Culture Media Inlet (M.IN); Microscopy Light window (MLW). (B) Blue color at MLW coming from the RGB LED iluminated reactor chamber (for example, blue exitation for carotenoid fluorescence).

3.2.4 Microreactor light control-light scattering and fluorescence detection system

To test the microreactor a data acquisition and control system was built (see Figure 3.20.)

The main idea was to have control over independent photoperiods and day and night cycles for microalgal culture in each chamber. In addition, there would be control over the intensity of light either for providing physiological stress for the microalgae or for normal growth conditions.There is alsocontrol of scattered light photosensors for microalgae density measurement and carotenoid detection in each culture chamber.

RGB LEDs in each chamber provided illumination for normal algal growth and for inducing stress responses. Additionally, a UV LED in each chamber was provided to augment the light-induiced stressing effect. RGB LEDs were also used to provide the light source for light scattering measurements, working in specific color modality (green or blue), as required. For measurement of cell concentration, for example, green light scattered by the cells in the microreactor chamber could be correlated to a change in light intensity detected by the photosensor located at 90 degrees with respect of the source of light. Furthermore, measurements (using blue exitation) of endogenous microalgal fluorescenc could also be detected using this 90 degree geometry.

There are 3 photosensors mounted in a external test platform (see Figure 3.21 A.) Each photosensor is a TCS3200 (TAOS INC, Texas, USA) programmable light-to-frequency integrated circuit with an 8 × 8 photodiode array with a total size of 1 mm X 1 mm (light sensitive area). Each TCS3200 is capable of converting the intensity of light of three different colors (red, green, blue) in a square signal with frequency proportional to light intensity (irradiance). This square signal is read by NI myDAQ counter input. Frenquency information (corresponding to light irradiance) is displayed in two different ways: using a LabView software based oscilloscope or a file data storing application also created using LabVIEW software.

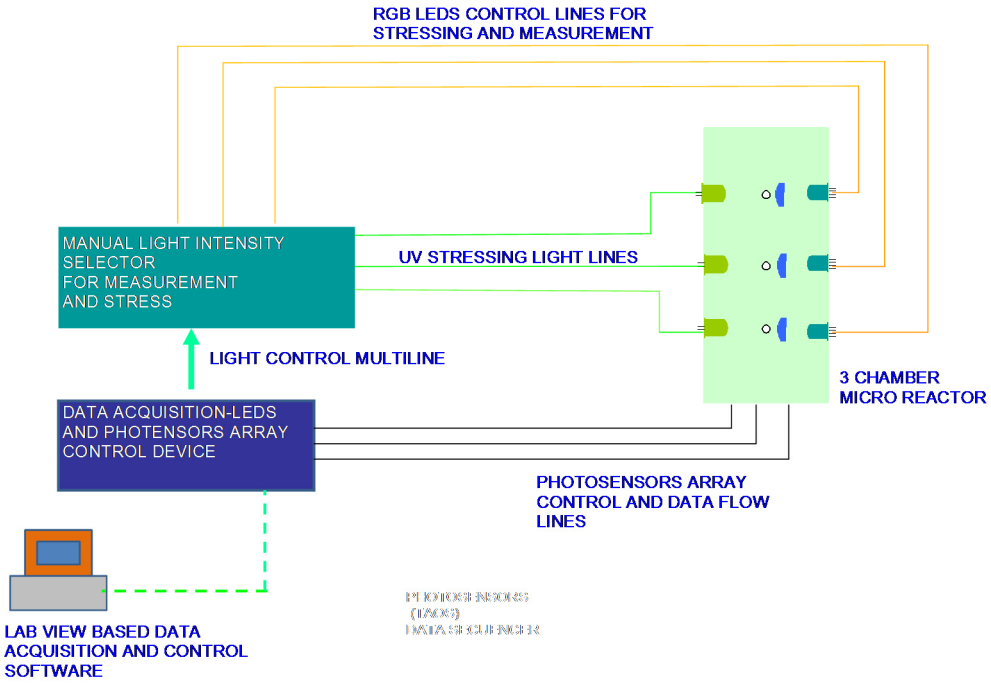

Figure 3.20 Microreactor light scattering-optical density and fluorescence detection system. The 3 photosensors array is mounted in a platform under the 3 microreactor device.

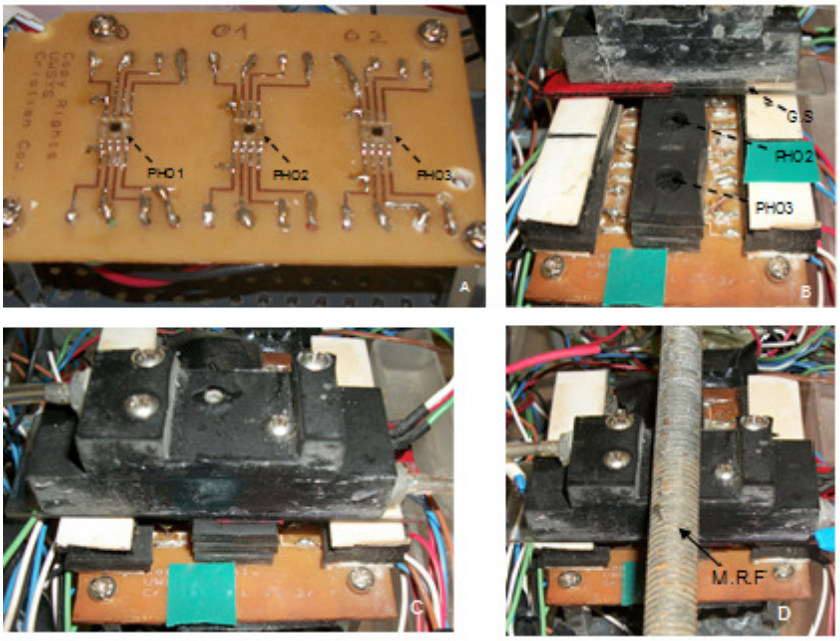

Figure 3.21 Photosensors array platform. (A) Photo sensors integrated circuits for each microchamber 1-2-3 (PHO1/2/3). (B) Enclosed photo sensors integrated circuits using punctured black rubber lateral light protection; glass slide (GS) aligned and resting on photosensor 1 (PHO1). (C) micro chamber reactor prototype aligned with photosensor 1. (D) Microreactor fixing rod (M.R.F.) after photosensor alignment. Rod mounted and fixed at each end , pressing down the reactor against photosensor.

A microreactor with a single complete chamber (mounted on photosensor 1) was fabricated. The 3 photosensor platform could accomodate 3 chambers, and so two of the photosensors, for chambers 2 and 3 were not used, but were available for future devices.

The microreactor device was mounted and aligned with its Microscopy-Photodetector window (M/D.W) and glass slide facing down (see figure 3.18 A, and 3.21 C) The TCS3200, with its 1mm by 1mm window, was mounted in an external platform, aligned and oriented toface upward, toward the M/D Window at the bottom of the microreactor. When the microreactor glass slide is mounted and aligned on top of the photosensor array some unwanted light entered from the external environment through the gap between the glass slide and the photosensor array printed circuit board. This gap

was due to the photosensor case thickness. To avoid light contamination that could affect the scattered light readings, black rubber material glued in layers was placed around the photosensor to reduce lateral incoming light (see figure 3.21 B.)

After the microreactor was carefully aligned with the photosensors, a frame set up with the help of a metal rod (see figure 3.21 D), pushing the microreactor down from the top of it, helped to keep the reactor in a fixed position without altering the alignment and causing problems with photosensors readings.

Light for both growing and stressing the microalgae was provided by 3-color RGB LEDs to produce white light, but the intensity of this light was varied depending of stress and growing cycle.

Cell concentration measurements in the microchamber using scattered light were carried out using only the green LED, with spectral output centered at 515 nm.

For fluorescence detection only the blue LED was used, with a spectral output centered at 480 nm.

Control/data acquisition for the-LEDs-photosensor array control system was controlled by NI MyDAQ hardware and NI LabVIEW software (National Instruments Corporation, Austin, TX, USA).

Light intensity of LEDs, (UV and RGB) was controlled manually, but automatic activation and deactivation of each color in the RGB led was software-controlled for growth, stress and detection sequences.

Timing control for day-night cycles, cell density and fluorescence measurement, multiplexing signals for photodetectors array control and data acquisition between the 3 chambers was executed with the control software.

The measurement system worked essentially in a serial mode. For microculture chamber 1 the measurement sequence started with cell concentration using light scattering, then a fluorescence measurement sequence was executed for the same chamber. The same two sequences of measurement,as mentioned earlier were repeated for microchambers 2 and 3. Each of these sequences has its own respective LED color and data acquisition sequence.

When measurement sequences for all of the micro chambers is finished, the period for normal growth light dose or stress light dose can be applied. After a period of light exposure is finished, the measurement sequence for the 3 chambers is repeated. The measurement cycle is repeated each 30 minutes and it takes 3 seconds per chamber.

3.3. Testing the microbioreactor

A number of tests were carried out to characterize microreactor performance. Three types of tests were performed:

- Macro tests: Tests were carried out using conventional macro methods with *Dunaliella sp* using culture flasks and a standard bench spectrophotometer.

- Microreactor fluidic system tests: Potential microalgal damage due to hydrodynamic forces, microchannel clogging, microalgae retention in the culture chamber, and agitation was assessed.

- Microreactor bioassay possibilities tests: The applicability of the microreactor as an effective biotest tool was assessed using microscopy and a microreacto-integrated optical system for measurement of microalgal growth rate and carotenoids. Conventional macro scale methods of flask-based culture were used as a reference.

These experiments were conducted to estimate time and materials required, costs, labor, and equipment as well as to identify technical problems inherent to conventional culture systems and thus having points of reference to compare the microreactor performance.

3.3.1. Macro tests

3.3.1.1 Specific Growth Rate in Culture Flasks

Dunaliella tertiolecta (CCMP1320, Bigelow, National Center for Marine Algae and Microbiota) was cultivated using filtered, UV-treated water from Taunton Bay, Franklin, Maine, at the Center for Cooperative Aquaculture Research, University of Maine.

Water pumped from Taunton Bay was treated using a 6-step process:

1. Sand filtration to retain particles greater than 100 microns.
2. UV light treatment with an industrial reactor (Trojan UV logic series, Aquafine Corporation) at an intensity of 13 mW/cm ^{2}.
3. Mechanical filtration through a 10 micron cartridge filter.

4. UV light treatment with reactor AST-120-2 (Emperor Aquatics).

5. Mechanical filtration through a 0.2 micron cartridge filter.

6. UV light treatment with an Emperor Aquatics 02040 reactor.

Shake flasks of 500 mL filled with 250 mL of the water purified as above, heat-treated for 15 minutes at 100°C, allowed to cool for 5 hours, and Guillards's 1975 F/2 Formulation (Proline Water Conditioner, part A and B, from Aquatic-Eco Systems, Inc. Apopka, FL) added to each flask, 40 µL part A - 40 µL part B.

Flasks were inoculated with vegetative microalgae to achieve an initial cell density of 222500 cells mL^{-1}. Cells were counted using a brightfield light microscope and haemocytometer (Hausser Scientific, Inproved Neubauer 0.100 mm depth) (see Figure 3.22) Salinity was measured (Extech Instrument, refractometer RF20) and found to be 35 ppt .

Flasks were injected with 0.45 µm filtered air (FTFE-Membrane, Whatman) for agitation and the for the introduction of CO_2 into the culture media. Cultures were incubated for 9 days at 22˚C under a light irradiance of 60 $\mu E/m^2s$ (14.23 Wm^{-2} considering 400-700 nm, PAR correlation of approximately 1800 $\mu E/m^2s$ = 427 Wm^{-2}), with a day-night cycle of 18 hours-6 hours respectively (Light meter, LI 250, LI-COR, USA). Cell concentration was determined every 48 hours, using a haemocytometer and the light microscope.

The specific growth rate of the flask-grown microalgae was determined from the exponential phase of algal growth using the following equation:

$\mu = \ln (N_2/N_1)/(T_2 - T_1)$

where μ is the specific growth rate (h^{-1}), N_2 and N_1 are cell concentrations at times T_2 and T_1 respectively.

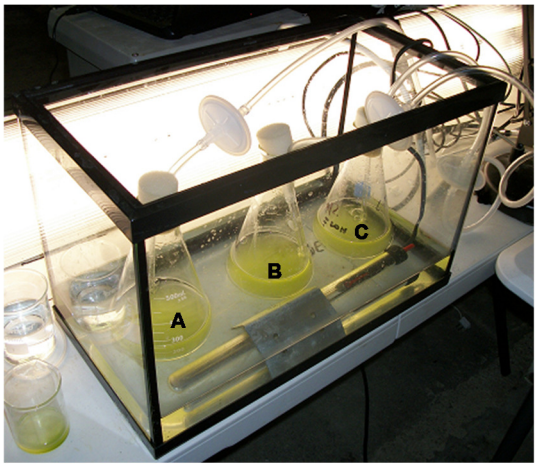

Figure 3.22 Set up for macro culture flask specific growth rate test. *Dunaliella tertiolecta* flasks A, B and C with same initial cell density: 222500 cell mL^{-1}. Flasks were incubated for 9 days at 22˚C under a light irradiance of 60 $\mu E/m^2s$ (14.23 Wm^{-2}, PAR correlation) with a day-night cycle of 18 hours-6 hours, respectively.

3.3.1.2 Culture Flask Carotenoid Extraction Test

3.3.1.2.1 Before stress cycle

Dunaliella salina used in this experiment was donated by Dr. Gary Wikfors from NOAA, Biotechnology Branch. Three 500 mL shake flasks labeled s1, s2 and s3 were filled with 250 mL of purified seawater.

Flasks were then heat-treated for 15 minutes at 100°C and allowed to cool for 5 hours. Guillards's 1975 F/2 Formulation (Proline Water Conditioner, part A and B, from

Aquatic-Eco Systems, Inc. Apopka, FL) was then added to each flask, 40 µL part A - 40 µL part B.

3.3.1.2.2 Osmotic stress

Salinity was measured with a refractometer (Extech Instrument, refractometer RF20), and the salinity of sea water media in the flasks measured 32 ppt. The medium in flasks s1, s2 and s3 was adjusted to 120 ppt, 170 ppt and 220 ppt NaCl, respectively .

After salinity adjustments, the 3 flasks were inoculated with vegetative *Dunaliella salina* that had been previously acclimated and grown with salinity of 120 ppt. Cells in the inoculum were counted using the brightfield microscope and a haemocytometer (Hausser Scientific, Improved Neubauer 0.100 mm depth). Cell density information was used to obtain the desired final concentration in the flasks. The starting cell density for the three flasks was 304166 cells mL^{-1} (see Figure 3.23 A.)

3.3.1.2.3 Light irradiance stress

Culture Flasks were incubated for 7 days at 23˚C under a light irradiance of 380 µE/m²s (90.14 Wm^{-2}, PAR correlation) under continuous illumination (Light meter, LI 250, LI-COR, USA). Flasks were shaken manually once a day. The cell density in each flask was determined every 48 hours by cell counting in the haemocytometer.

3.3.1.2.4 Pigment extraction and analysis

At the start of the culture period (day 0) and at the end of stress period (day 7) samples of 4 mL were taken from each microalgae flask s1, s2 and s3. Each of these samples were concentrated by centrifugation at 5000 rpm for 5 min.. The liquid phase was extracted after centrifugation and the remaining cell pellet was mixed with 4 mL of acetone/water (80:20 v/v). The mixture was vortexed for 3 minutes to improve pigment extraction.

An additional centrifugation at 5000 rpm for 5 minutes was carried out and only the liquid phase was extracted from the tubes and placed in new glass 10 mL containers in preparation for spectrophotometry This last process was carried out under illumination at very low light intensity to minimize photopigment damage (see Figure 3.23 B). The pigment extraction protocol is based on that of Lichtenthaler [20], which also details equations used for quantitative determination of total chlorophylls and carotenoids after solvent extraction and spectrophotometric data (Hatch Odyssey DR 2500 Spectrophotometer).

Absorbance measurements were acquired at 663.2 nm; 646.8 nm and 470 nm and repeated for each 4mL extraction sample coming from flask s1, s2, s3.

These absorbance were used as input into the following equations to determine the relative quantities of chlorophylls and carotenoids.

$$Ca = 12.25\ A663.2\ - 2.79\ A646,8$$

$$Cb = 21.50\ A646.8 - 5.10\ A663,2$$

$$C\ x+c = (1000\ A470 - 1.82\ Ca\ - 85.02Cb) / 198$$

Where C*a* and C*b* are Chlorophyll *a* and *b* concentrations respectively (µg/mL of extract solution), C *x+c* is total carotenoid concentration (µg/mL of extract solution), *A* is the absorbance reading at the wave length indicated by the subscript.

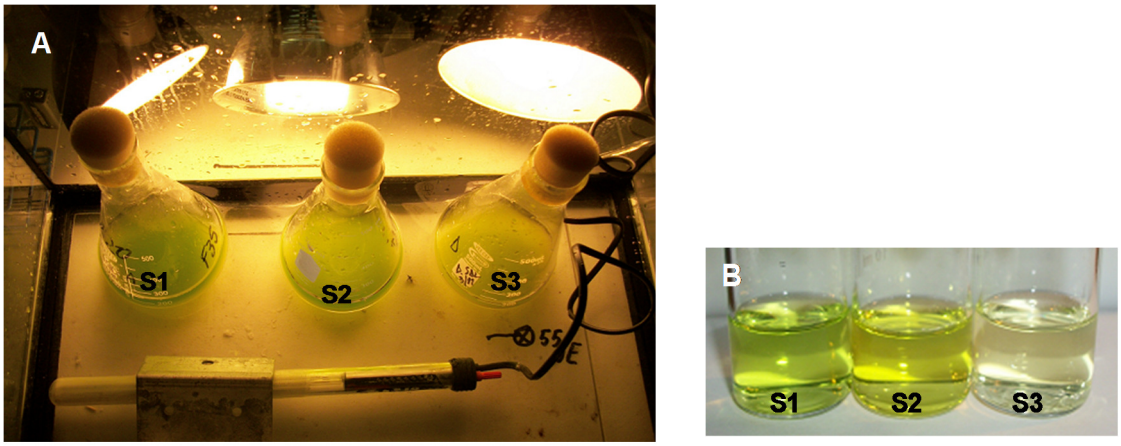

Figure 3.23 *Dunaliella salina* culture under osmotic and light irradiance stress. (A) 7 day period, 23˚C, continuous light irradiance of 380 µE/m²s (90.14 Wm^{-2}, PAR correlation), S1,S2,S3 with salinities: 120 ppt, 170 ppt and 220 ppt respectively ; (B) Pigment extraction after stress period in 10 mL containers for spectrophotometric analysis.

3.3.2 Microreactor fluidic system tests

Prior to the microfluidic tests, the microreactor was washed 4 times with deionized water, injecting water through the inlet port twice using a 1/16 inner diameter

-1/8 outer diameter Tygon R-3603 plastic tube (1.58 mm and 3.1 mm OD) and twice through the outlet port, being careful to completely empty the fluidic system. Deionized water was injected using a 10 mL syringe (BD, Franklin lakes, NJ) connected to the tubing. The reason for injecting deionized water from both the inlet and the outlet was the need to rinse the microalgae retention mesh located inside the reactor.

The same procedure before was used for the reactor disinfection using 95% ethanol instead of deionized water, and having 40 seconds as a retention time for each ethanol injection to increase disinfection contact. Sterile deionized water was used to rinse the chamber 4 times, both from inlet and outlet, and then the microreactor was rinsed with sterilized sea water in preparation for fluidic tests.

3.3.2.1 Microalgae damage test

This test was designed to observe the response of microalgae to hydrodynamic forces inside microchannels and culture chamber, and to monitor any cell damage due to shear and pressure changes, as well as potential aggregation and resulting channel blockage.

A 50 mL of sample was withdrawn from a 250 mL *Dunaliella tertiolecta* flask culture. Cells were counted using the light microscope and a haemocytometer (Hausser Scientific, Inproved Neubauer 0.100 mm depth). Using sterilized sea water media, cell density was adjusted to reach a value of 300000 cells mL^{-1}. An image of initial cell morphology was acquired from a 50 µL sample on a glass slide from this adjusted

concentration, using an inverted microscope (Nikon Eclipse Ti) with integrated camera and imaging software (Spot imaging solutions, Diagnostic Instruments, Inc).

Another sample of 500 µL from the same dilution of 300000 cells mL^{-1} was injected into the chamber inlet at a rate of 5 µL min^{-1} using a 10 ml syringe (BD, Franklin lakes, NJ) and the syringe pump (New Era pump systems Inc, NE-300) through the 1.58 mm ID plastic tubing.

Again, microscopic images and real time observations were acquired from the bottom microchamber window to compare the cell morphology before inoculation and after the cells arrived in the microchamber (see figure 3.24).

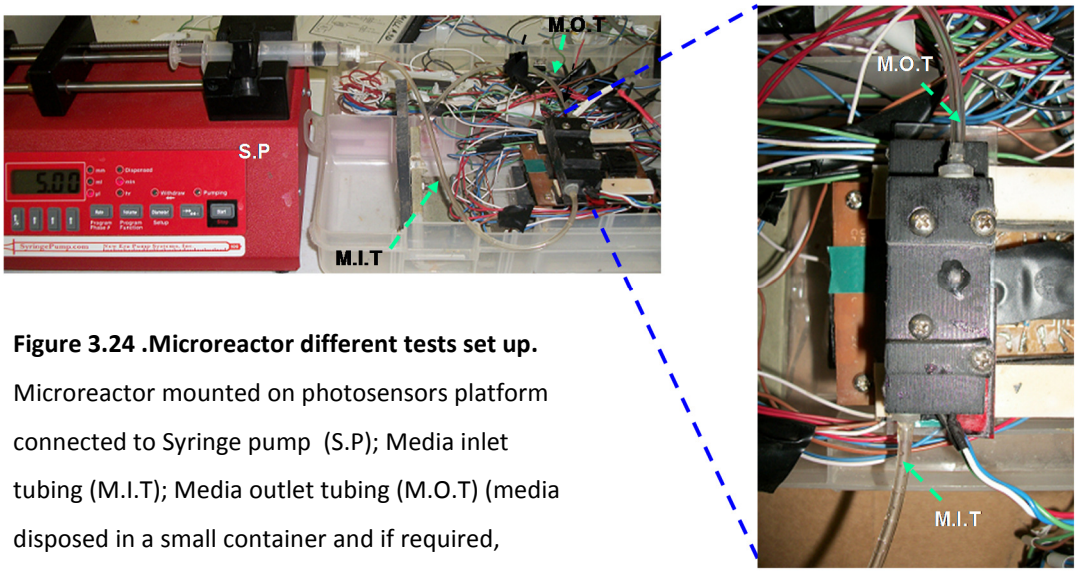

Figure 3.24 .Microreactor different tests set up. Microreactor mounted on photosensors platform connected to Syringe pump (S.P); Media inlet tubing (M.I.T); Media outlet tubing (M.O.T) (media disposed in a small container and if required, collected for cell morphology or counting).

3.3.2.2 Microchamber retention mesh and agitation system effectiveness test

This test was performed to observe microalgal retention by the mesh located at microchamber outlet and also to evaluate the efficacy of cell agitation resulting from the incoming media of flow at the bottom of the chamber. The inlet, outlet and microreactor were rinsed 4 times with deionized water, followed by sterilized sea water to ensure that all microalgal residue from the previous experiment was removed., A 50 mL sample was taken from a 250 mL *Dunaliella tertiolecta* flask culture and adjusted to a cell density of 2000000 cells/mL.

Cells were counted using light microscopy and haemocytometer (Hausser Scientific, Inproved Neubauer 0.100 mm depth) and dilutions adjusted using sterilized sea water medium. A 500 µL sample of the same dilution of 2000000 cells mL^{-1} was injected into the chamber inlet at a rate of 5 µL min^{-1} using a 10 ml syringe(BD, Franklin lakes, NJ) and the syringe pump (New Era pump systems Inc, NE-300) through the 1.58 mm ID plastic tubing. Samples were collected at the outlet of the microreactor and cells were counted in the haemocytometer. The same configuration for the microalgal damage test (syringe pump-microreactor), was used for this test (Figure 3.24).

Incoming media passing through the micro chamber bottom inlet and channel blockage were monitored.

3.3.2.3 Surface retention test

Using one of the semitransparent material prototypes, a cross section of one of the internal microchannels is exposed using a cutting plane parallel to the direction of

the pipe. This physical cut was made using a grinding tool (Dremel, Racine, WI, variable, speed rotary tool), exposing the internal surface of the microchannel for close examination and testing. The material was thoroughly rinsed with distilled water after the grinding process.

Images of the rinsed and dried cross section were obtained with a stereo microscope (Leica EZ4D) (see figure 3.25). The exposed section was inoculated with 30 µL of microalgae taken directly from the original 250 mL *Dunaliella tertiolecta* flask culture. The surface tension of the fluid kept the exposed surface of the micropipe wet even when it was held upside down for inspection in the inverted microscope. Microscopic images of microalgae on the surface of the exposed microchannel, and also on the surface of one of the inlets were obtained for further analysis.

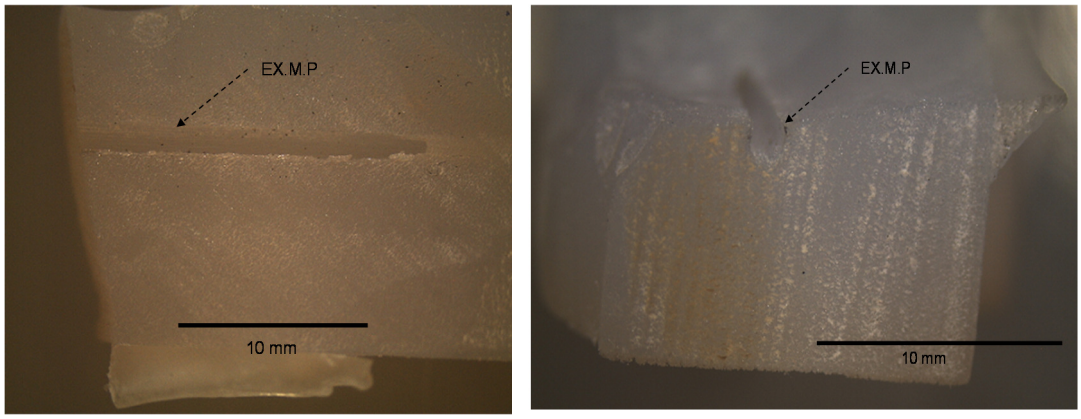

Figure 3.25 Exposed microchannel (EX.M.P). Left and right figures (longitudinal and cross section, respectively) show different views of a 1 mm diameter microchannel internal surface obtained by grinding the material until reaching microchannel depth. The microchannel surface was inoculated with microalgae to observe fluid and microalgal behavior.

3.3.3 Microreactor biotests

The objective of these tests was to determine the potential for using the microreactor as a tool for microalgal biotests, either employing microscopy or the integrated optical detection system in the microreactor for measurement of optical density and fluorescence.

Before microreactor tests could be performed, several parameters were adjusted, including automatic diurnal photoperiod sequence, light intensity for normal growth and detection, sequences of green and blue illumination for activation, measurement protocols, and photodetector activation and reading status for each of the chambers.

3.3.3.1 Scattering calibration and response to cell density

The cell density (cell mL^{-1}) measuring system, based on scattering of green (515 nm) light, was calibrated as follows:

Using a serial dilution procedure four suspensions of *Dunaliella tertiolecta* at different concentrations were prepared using pure culture media and cells obtained from a culture at the end of its exponential growing phase,.

Suspensions contained: 1996000, 1068000, 636000, 364000 and 0 cell mL^{-1}. Samples were stored in test tubes. The microreactor was cleaned and prepared using the procedure described in 3.3.2.

After cleaning procedure, the reactor was mounted and aligned on the photosensor array platform, covering any other extra source of light than the one coming

from the microchamber, and using the threaded rod to keep the reactor in a fixed position regardless of movement in the media tubing, avoiding misalignment of the photosensor (see Figures 3.21(B) and 3.21 (C)).

140 µL samples of each microalgal suspension were injected into the microreactor. The reactor was flushed with clean culture medium prior to injection of each sample. Green light alone was activated and the signal frequency from the photosensor was measured using a data acquisition system and a simulated oscilloscope, both controlled via LabView (National Instruments, Austin, Texas, USA). This photosensor generates pulse frequency that is proportional to irradiance of scattered light.

3.3.3.2 Microscopy calibration and cell density measurement

After scattered light calibration, remaining algal cells were flushed out with fresh media. The reactor was moved from the photosensor platform to an inverted microscope (Nikon Eclipse Ti- SR, Japan- RT3 CCD digital camera, SPOT imaging). Using the same *Dunaliella tertiolecta* samples prepared for scattered light tests, 140 µL of each sample was injected into the microreactor.

Microscopic images of each sample were taken using a 20X objective . The microscope was focused at the half-way point between the bottom of the culture microchamber and the top of the microreactor (1 micron mesh) to a have acquire a representative image of the microalgae in the microchamber (see figure 3.26). Standardized image region dimensions (frames) were used for visual cell counting (cells/frame) to create a calibration with sample density (cells mL^{-1}).

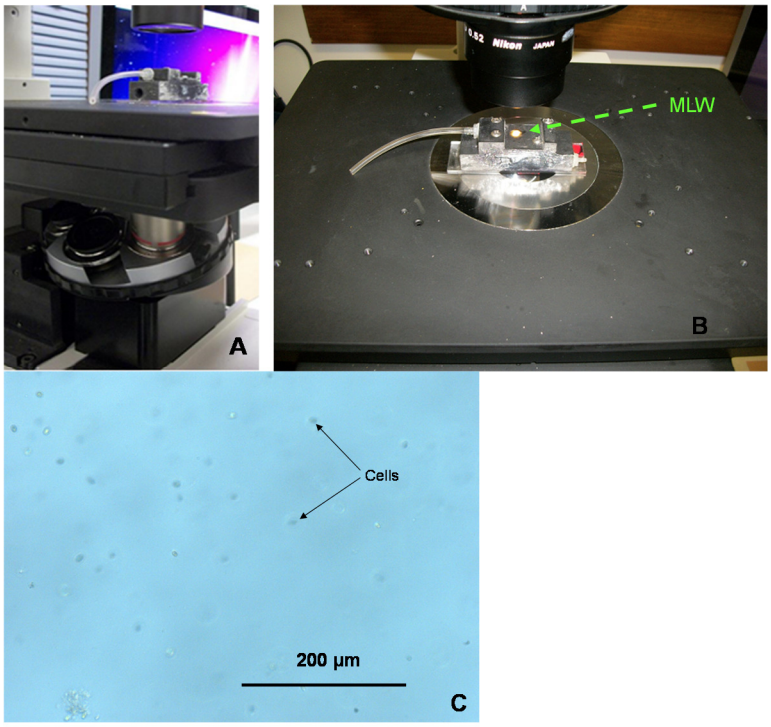

Figure 3.26 Microscopy calibration for cell concentration determination. (A) Microreactor placed on inverted microscope. Objective 20x facing microscopy-photodetector window at the bottom of the glass slide; (B) Light source entering from top of the reactor (MLW); (C) standard calibration. image of *Dunaliella tertiolecta* cells in the microchamber (standard frame used for cell counting).

3.3.3.3 Microreactor specific growth rate test

The microreactor was disassembled and microreactor parts A and B were washed and debris were flushed out by injecting deionized water . A new retaining 1 micron mesh was installed. Parts A, B and mesh were assembled, sealed using clear silicone (Loctite® Clear Silicone waterproof sealant) and allowed to cure for 24 hours. Ethanol (95%) was

used to disinfect the microchamber by, injecting it into inlet and outlet. Four consecutive rinses were executed, then deionized water was injected into the inlet and outlet.

Seawater medium was prepared using the same method as in 3.3.1.1, but in this case just one 500 mL flask was filled with 250 mL for sterilization and the Guillards's 1975 F/2 Formulation was added using 105 µL part A - 105 µL part B.

Regular CO_2 present in the air was added to the culture media flask by injecting filtered air (0.45 µm filter), for reducing potential contamination.

Initial readings of temperature, pH, salinity, O_2 and CO_2 were taken after 6 hours of air injection into the media flask.

The microreactor was mounted and aligned on the photosensor platform. The RGB LED control system was adjusted for a photoperiod of 18 hours of light/6 hours of darkness with Irradiance of 40 µE $m^{-2}s^{-1}$ (E = $6.023x10^{23}$ quanta, 9.48 Wm^{-2} PAR correlation) using red and blue light.

140 µL of *Dunaliella tertiolecta* from a culture flask in the exponential growing phase were injected into the reactor microchamber at rate of 5 µL min^{-1} using a 10 ml syringe (BD, Franklin lakes, NJ) and the syringe pump (New Era pump systems Inc, NE-300) through the 1.58 mm ID plastic tubing. After the microalgal sample was injected, a new 10 ml syringe was used to inject 70 µL of seawater medium (day 0), taken from the 500 mL aerated flask at a rate of 5 µL min^{-1}. Observations of cells were made with a light microscope using a 10 X objective (Nikon Labophot, Japan). The microreactor was then moved to the inverted microscope. Images were acquired using a 20X objective . The

microscope was focused half way between the bottom and the top of the culture microchamber to obtain a standard image frame for cell counting (cells/frame) for cell density correlation (cell mL^{-1}). Additional images using 4X and 40X objectives were acquired.

The microreactor was moved back to the photosensor platform and the Inlet/outlet fittings were connected to their respective micropump and disposal lines. The photoperiod of 18 hours of light/6 hours of darkness with Irradiance of 40 µE $m^{-2}s^{-1}$ was activated and photosensor measurements for cell density correlation were acquired.

Temperature in the reactor was regulated basically by the LED heat (at 40 µE $m^{-2}s^{-1}$, 9.48 Wm^{-2} PAR correlation) and room stable temperature maintained by air handling unit with automatic heating and colling features. The resultant temperature was previously checked to be within the normal growing range for *Dunaliella sp.* [21] [22].

Each 24 hours, the same cycles of microscopy observations, standard pictures, pumping of new media (nutrients, CO_2, N among others) and light intensity measurements were performed.

For each trial new culture media with nutrients were added to the microreactor using doses of: 10, 20, 40, 40 µL for days 1,2,3 and 4 respectively, with a pumping rate of 5 µL min^{-1}.

After the first microreactor trial, several additional trials were performed to find conditions for the optimal growth rate, using the same data acquisition cycles and protocols as the original trial.

CHAPTER 4

RESULTS

4.1 Microreactor manufacturing

A single chamber microreactor was successfully built and tested (see figure 4.1).

The microdevice consisted of two photopolymer-assembled main pieces, A and B, both fabricated using an additive manufacturing process (3D printing) based on a UV curable jetted photopolymer material and a nontoxic support material. The culture microchamber had a capacity of 70.33 µL and was built with two light windows on each side, one for normal growing/stressing light conditions and the other for UV light used for inducing stress. These windows were 3.46 mm in diameter and internal cylindrical channels were 1 mm in diameter. The material chosen for the reactor was Vero™ Black (supplier?) since it eliminated excessive light transmittance, which affected the scattered light detection system.

The device was 60 mm x 21.9 mm x 19 mm, weighing 49 gm (considering only photopolymer material) and was manufactured in 1 hour and 49 minutes.

The device cost, including photopolymer and support material, for pieces A and B was 47.30 $USD.

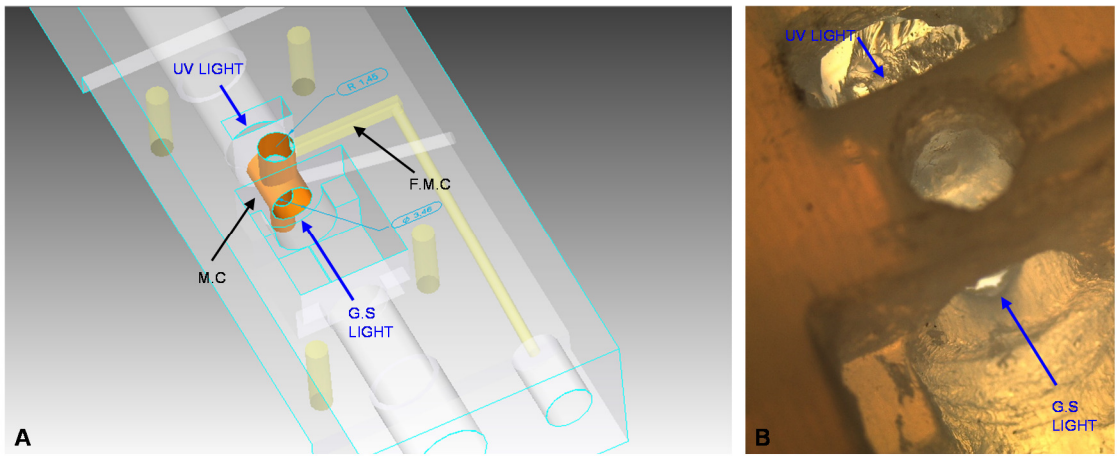

Figure 4.1 Bottom views. Design and print of first semi transparent material prototype, figures A and B respectively, showing 1.45 mm (radious) window for photodetection and microscopy and 2 windows of 3.46 mm in diameter, one for UV stress light (UVLight) and the other for stress/growth RGB light (G.S Light). Microchamber (orange) (M.C); Fluidic microchannel (F.M.C). Final device was identical but it was built using black material (Vero™ Black).

Major challenges in the fabrication and assembly processes were the cleaning of support material from microchannels and the sealing of windows to prevent culture media leakage.

Cleaning of the microchannels was achieved by pushing support material out with a wire of the same diameter as the microchannel, since water jetting and hot water sonication were unable to remove this material. Microchannel internal surface quality after this cleanning is addressed below. The UV window was sealed using optical cement and the growth/stress light (RGB LED) window was sealed using a collimator lens and optical cement. The quality and strength of the optical cement/photopolymer material joint was not subject to leakage.

Assembling of part A, the retaining micromesh, part B, screws and bottom glass slide was simple and straightforward, but the curing time for clear silicone (24 hours) used for sealing the micromesh with part A-B, and for the glass slide at the bottom, extended the time required before the reactor would be ready for use.

4.2 Macro test results

4.2.1 Specific growth rate

Dunaliella tertiolecta was cultivated in shake flasks for 9 days .

Cell concentration data are presented in Figure 4.2 which represents the mean of the cell density in the three flasks. An interval from day 2 to day 8 was used for calculation of net specific growth rate (μ) using the equation specified in 3.3.1.1. μ was 0.01 h^{-1} and the doubling time (Ln2/ μ) was 69.3 hours.

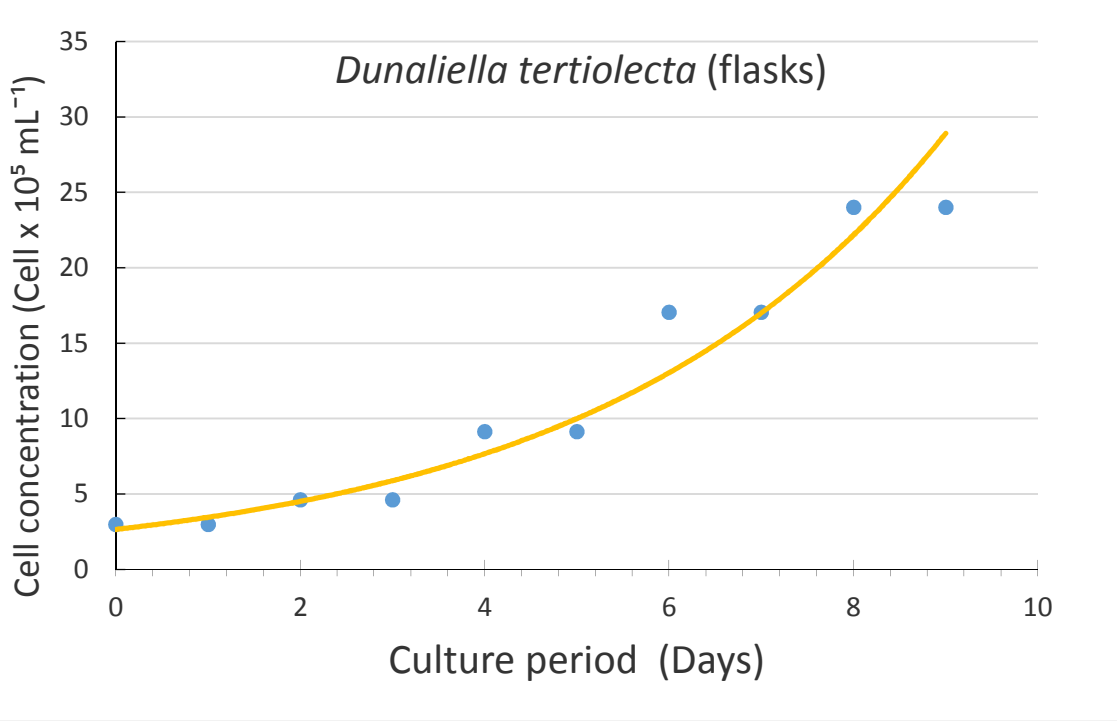

Figure 4.2 *Dunaliella tertiolecta*, flask culture. The plot represents the mean value of cell concentration in three flasks, A, B and C, inoculated to the same initial cell density: 222500 cells mL^{-1}. The flasks were incubated for 9 days at 22˚C, salinity 35 ppt, under a light irradiance of 60 µE/m^2s (14.23 Wm^{-2} PAR correlation) with a day-night cycle of 18 hours-6 hours, respectively.

4.2.2 Carotenoids extraction

Three flasks of *Dunaliella salina* were cultured according to the protocol in 3.3.1.2 for a period of 7 days under different high salinities: 120 ppt, 170 ppt and 220 ppt and one high light irradiance level, for comparing intracellular carotenoid production and the effects of different stressing environments. For each flask, initial and final cellular concentration and carotenoid content (using solvent extraction method and spectrophotometry) were obtained (see Figures 4.3, 4.4 and 4.5.)

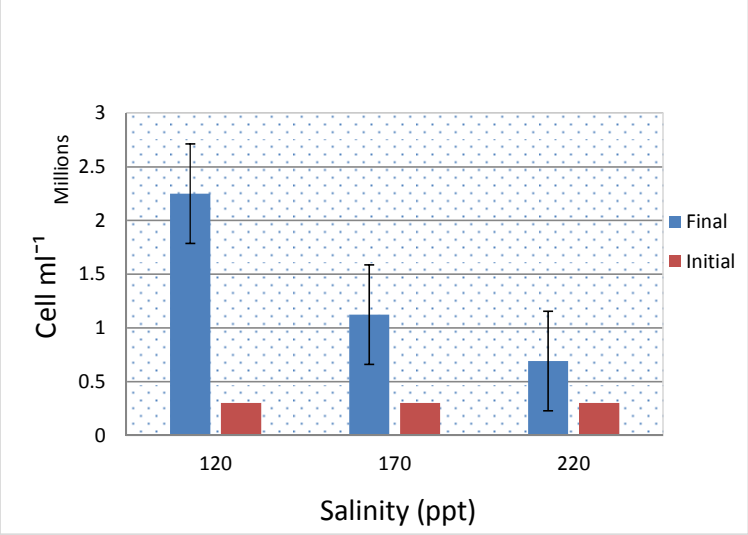

Figure 4.3 *Dunaliella salina* cultured during 7 day stress period in flasks. Cell concentration after growing under high irradiance of 380 µE/m²s (14.23 Wm^{-2} PAR correlation) and high salinity conditions (120, 170 and 220 ppt) at 23˚C.

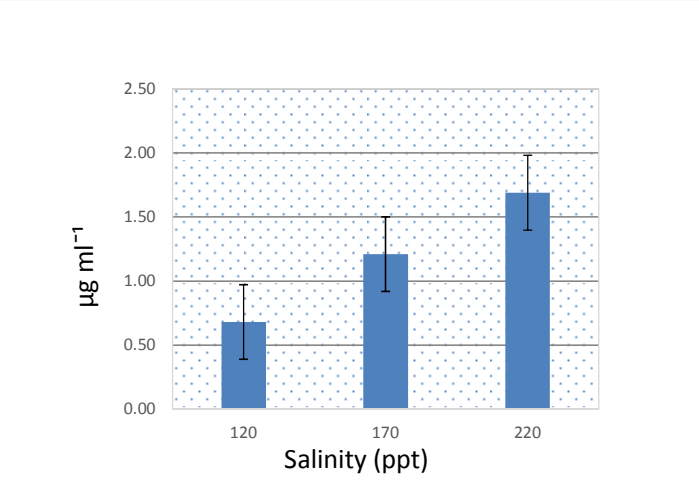

Figure 4.4 Carotenoid production in *Dunaliella salina* after 7 day stress period. High irradiance of 380 µE/m²s (90.14 Wm^{-2}, PAR correlation) and different high salinity conditions (120, 170 and 220 ppt) at 23˚C.

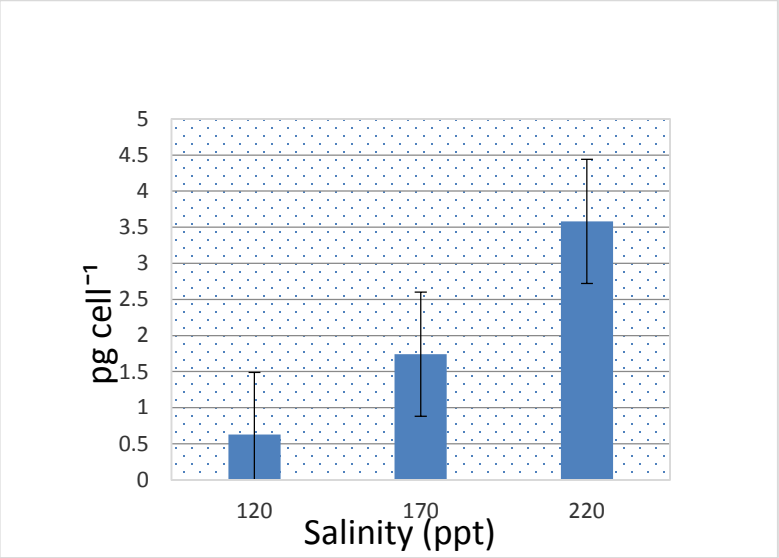

Figure 4.5 Final Carotenoid concentration (pico grams cell^{-1}) in *Dunaliella salina* flask culture. 7 day stress period with high irradiance of 380 µE/m²s (90.14 Wm^{-2}, PAR correlation) and high salinity conditions (120, 170 and 220 ppt) at 23˚C.

4.3 Microreactor tests

4.3.1 Microalgae damage test

Two images of *Dunaliella tertiolecta* were obtained to assess possible damage caused by excessive pressure or fluid shear force during injection into the microreactor chamber through the microchannels. The first image was obtained from a microalgal sample placed on a microscope slide before pumping microalgae from the same culture with a syringe pump, into the microchamber at a rate of 5 µL min^{-1} using a 10 ml syringe. The second image of the inside the microchamber was acquired,from the bottom window.

No apparent abnormalities (disrupted cells for example) between the pre-injected and post-injected microalgae were observed. See figure 4.6

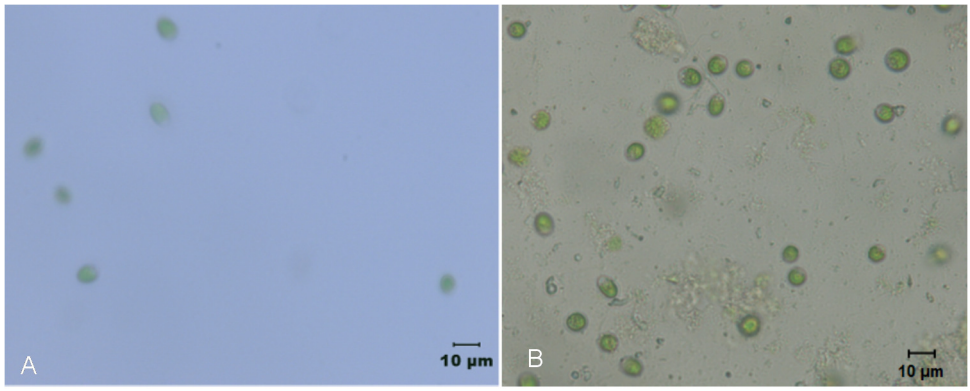

Figure 4.6 Images of *Dunaliella tertiolecta* cells. Before and after (A and B respectively) being pumped into the microchamber. Pumping rate: 5 µL min^{-1}, using a 10 ml syringe.

4.3.2 Retention mesh and agitation system

Microalgae at a density of 2×10^6 cells ml^{-1} were pumped into the microchamber, using a 10 ml syringe mounted on the pump and set to a dispense rate of 5 µL min^{-1}. At the same time,at the microreactor outlet culture medium was collected and observation and counting of cells was carried out to check for cell leakage.

Cells were observed at the outlet media, therefore cells were not 100% retained by the 1 µm mesh.

The percentage of micromesh capacity for retention of *Dunaliella sp* was calculated as follows:

$$\% \text{ retention} = 100 \times \frac{(C_{in} \times V_{in} - C_{out} \times V_{out})}{C_{in}}$$

Where C in is microalgal concentration at the inlet port, V in is the volume of media pumped taking the starting point when the medium has already crossed the 1 µm mesh at the reactor and is present at the outlet port, but has not yet been delivered, Cout is the microalgal concentration in the sample obtained at the outlet port and Vout is the volume collected at the outlet port. The value found for retention was 36.3%.

The agitation system, based in the incoming flow of media at one side of the bottom of the reactor, was observed but not quantified. The incoming medum moved the surrounding cells in the incoming flow area at the bottom but hydrodinamic forces were not able to cause a complete change in cell´s positions in the whole chamber volume, particularly those at the bottom of the reactor touching the glass slide window.

This behavior corresponds with theory in microfluidics expressing difficulties in agitation processes in laminar flow characterized by Reynolds numbers Re less than 2300.

Pumping rates of 10, 20, 35 and 50 µL min^{-1} were selected.

Considering that the microculture chamber is a 2.9 mm diameter cylinder, and the flow direction is from bottom to top, we obtained Reynolds numbers for flow rates

from 10 to 50 µL min^{-1} using the following formula:

$$Re = \frac{D \times V \times \rho}{\mu}$$

where D is hydraulic diameter, V is the fluid velocity based in the cross section of the pipe, ρ is fluid density and μ is dynamic viscosity. Table 4.1 shows the values obtained. Here we can see that values for Re are extremely low confirming that of flow media in the chamber is laminar.

µL min^{-1}	Re
10	0.08
20	0.16
35	0.28
50	0.4

Table 4.1 Reynolds for media flow inside the microchamber at different flow rates. Calculations assumed sea water salinity of 31 ppt and temperature 27°C.

4.3.3 Surface Retention

Different pictures were taken to check possible cell retention by the photopolymer surface and also to check the quality of this surface for this type of application. The quality of this surface also could be affected, to some extent, by the method for extraction of support material after the printing process. A small amount of cell retention was observed but not quantified.

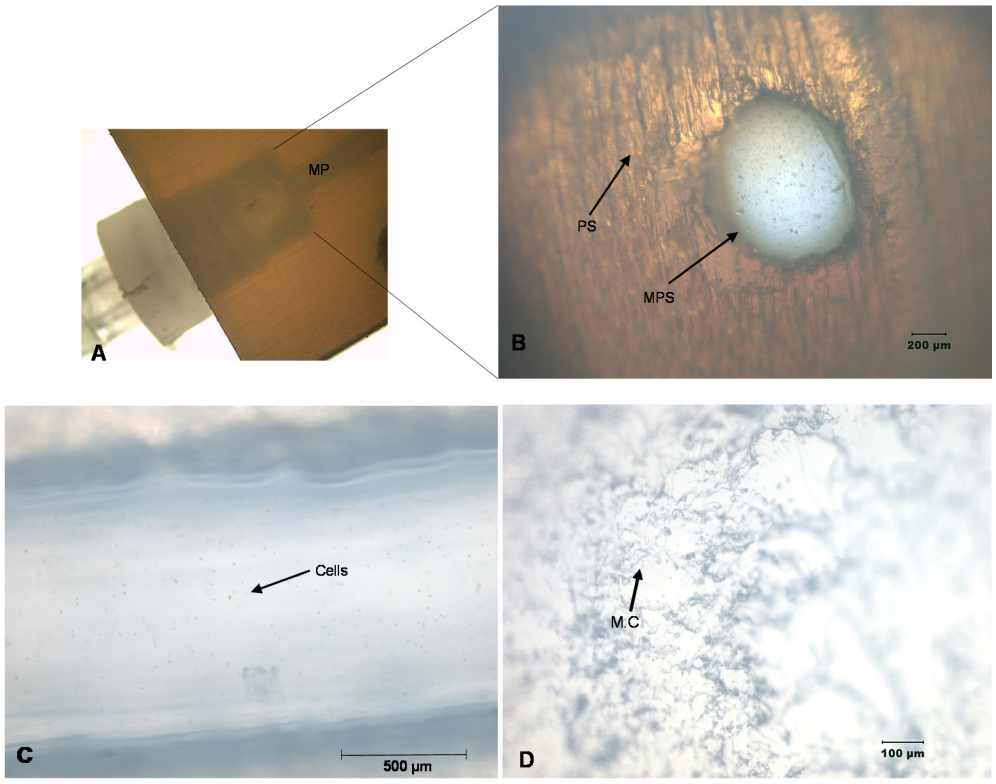

Figure 4.7 Surface retention test using *Dunaliella tertiolecta* cells. (A) Microreactor inlet for microalgae and culture media showing section enhanced in B; Microchannel (MP); (B) Microchannel circular section picture taken without the plastic threaded tubing connector; Microchannel section (MPS) showing *Dunaliella tertiolecta* cells inside the channel floating in the media; 3D printer photopolymer surface details (PS); (C) Microchannel longitudinal cut, cells can be seen floating inside of it; (D) Microalgae cells (M.C) retained by the internal inlet surface cavities created by deposition of photopolymer layers in the 3D manufacturing process.

4.3.4 Light scattering measurement

Changes in signal frequency from the photodetector array system located at the microreactor bottom window were detected when 6 samples of different microalgae cell concentrations were injected into the chamber. Changes in frequency were proportional to light irradiance at 515 nm. Scattered light coming from the reactor was detected at 90

degrees with respect to the light source and correlated with changes in microalgal cell concentrations. Light irradiance was expressed as relative intensity and this value was proportional to the cell concentration inside the chamber.

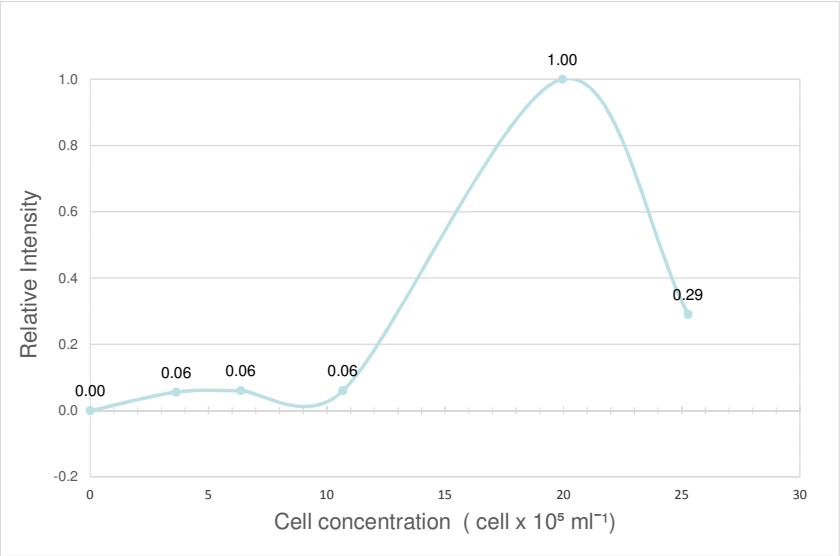

Figure 4.8 Scattered light detection system for cell density measurement using *Dunaliella tertiolecta*. Photodetector array frequency signal proportional to scattered light (intensity). Light source: Green LED 515 nm. Lack of correlation between relative intensity and microalgae concentrations higher than $20x10^5$ ml^{-1} is observed.

4.3.5 Microscopy and cell density

A correlation curve was built between microscopy counting using a standard frame area for each sample and values of cell concentration from the same samples obtained by haemocytometer counting. This calibration curve was lineally adjusted to be used for further microscopy counting directly from the reactor bottom window.

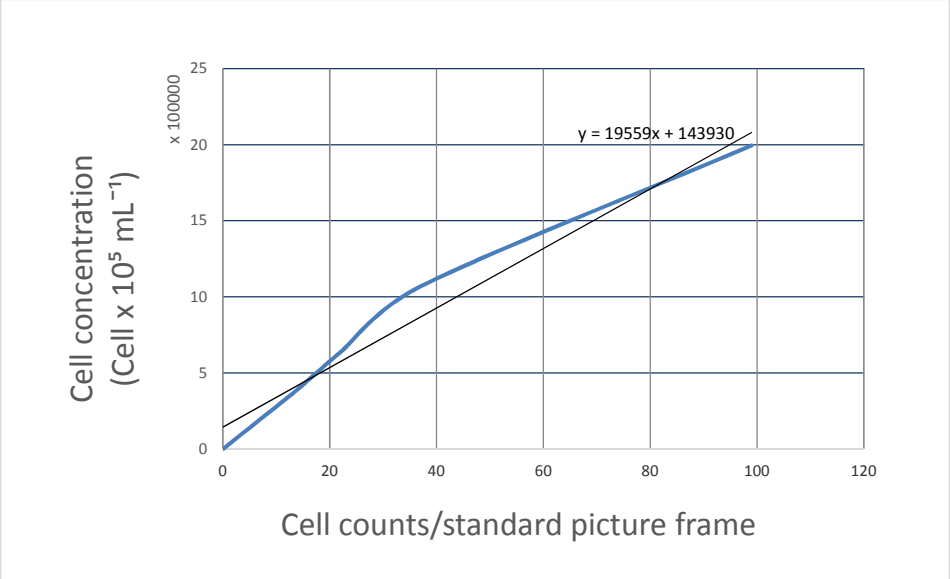

Figure 4.9 ***Dunaliella tertiolecta*** **microscopic images and cell counts.** 20x objective and standard image frame (area: 251313 µm²). The linear equation is used for further cell concentration measurements.

4.3.6 Specific Growth rate

Eight *Dunaliella tertiolecta* growth tests were carried out using the microreactor as a culture device. None of the eight tests showed signs of cell replication in the microchamber, and all of them showed fast progressive population decline.

3 growth tests showed the longest period for reaching minimum population or survival after 2 and 4 days (cells at the bottom of the microchamber with low motility were observed).

The calibrated growth curve using the standard image frame from 4.3.5 was used for microalgae counting and assessment of microreactor culture chamber.

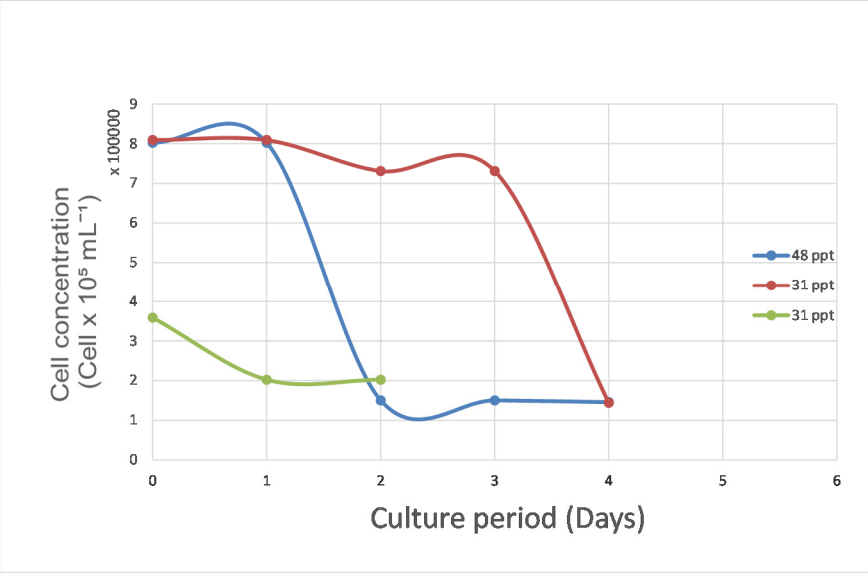

Figure 4.10 Microreactor growth tests using *Dunaliella tertiolecta*. Cell counting was performed using a 20x microscope objective, standard image frames and the calibration equation. Three tests shown here indicate no signs of cell replication and instead display a progressive decline of cell population in the microchamber. Salinity was adjusted to 48 ppt and 31 ppt to test any possible effects on survival.

CHAPTER 5

DISCUSSION

5.1 Microreactor fabrication

A 3D-printed microreactor measuring 40 mm X 21.9 mm X 19.03 mm was successfully fabricated. Some of the device's internal structures fall within the microfluidic domain while other features were of larger dimensions. The fluidic system was composed of microchannels 1 mm in diameter and the culture media was pumped into the microreactor at rates in the range of microliters. The 70.33 µL microculture chamber was successfully sealed to eliminate fluid leakage between the two LED access windows (UV and RGB LEDs) and the glass slide bottom window. The 1 µm mesh on the top of the chamber allowed exchange of culture media while retaining the majority of microalgal cells.

The presence of support material in the 3D printer fabrication process was a limiting factor in creating sub-millimeter scale enclosed structures, specifically microchannels for media inlet and outlet. Support material could not be removed from inside of 1 mm width microchannels by jetting water under pressure even if the fabricated device was pre-treated in a heated ultrasonic bath. Microchannels were ultimately freed from support material using a stiff wire to push the material out of the channel. It has been reported that the 3D printing process can be carried out without support material in enclosed designs, such as 800 µm diameter circular channels [9], but this process was not attempted in the present work.

A support material that is soluble in solutions of NaOH has been recently released by Stratasys under the trade-name SUP706. This option could be more effective for creating smaller microchannels, but the removal step is limited by diffusion [39].

The final microreactor device color was black to reduce light interference in the light scattering-based cell concentration measuring system. At the same time one disadvantage of this color was that it did not allow direct observation of fluid flow. The final microreactor design permitted assembly and disassembly for cleaning, disinfection and retention mesh replacement.

5.2 Macro tests

Macro tests using microalgal cells in flasks provided points of reference for tests in microchambers. The basic goals of microreactor fabrication were the reduction of size, materials (hardware, nutrients, culture media, etc.), time, and labor, for carrying out cultivation and testing of microalgal cultures.

Dunaliella tertiolecta was cultured in flasks during a 9 day period at 22˚C and under a light irradiance of 60 $\mu E/m^2s$ (14.23 Wm^{-2} PAR correlation) with a day-night cycle of 18 hours-6 hours, respectively, reaching a specific growth rate of $\mu = 0.01\ h^{-1}$ and doubling time = 69.3 hours. Carotenoids were extracted from *Dunaliella salina* after stressing the cells by exposure to different salinity and light conditions over a 7 day period.

Maximum intracellular carotenoid concentrations correlated with the maximum tested salinity, 220 ppt, and exposure to light at 380 µE/m²s (90.14 Wm^{-2}, PAR correlation) and 23˚C. In both cases, microalgae population growth occurred and carotenoids were produced in concordance with past reports.

5.3 Microalgae damage

No apparent cell damage was observed after injection of microalgal cells into the culture chamber. During normal injection of culture media using the fluidic pump and after cells were placed inside the chamber, a cyclical and short increase/decrease in pressure was observed by microscopy via the reactor bottom window. In this way a sudden burst was created, moving the cells apart after reaching a pressure peak. A plausible explanation for this phenomenon was that an accumulation of cells at the top 1 µm mesh, pushed by the ascending flow from the bottom inlet, was blocking the normal medium flow until a peak where the pressure is released and the media could flow again to the outlet, initiating this pressure cycle again.

5.4 Retention mesh and agitation system

Nylon retention mesh with openings of 1 µm, did not retain 100% of the microalgae. *Dunaliella sp* lacks a rigid cell wall and has an average size of 5 to 25 µm in length and from 3 to 13 µm in width and it can change its shape from rod to ovoid according to environmental conditions. Nevertheless, the reason that cells escape from the chamber is not clear. Two different hypotheses may explain this, one is the imperfections in the putative 1 µm mesh, with pore or openings sizes different to

manufacturer specifications statement and the other refered to plasticity of *Dunaliella sp* due to the lack of a cell wall with the possibility of being squeezed through mesh imperfections when the culture is injected and the pressure inside the chamber is increased. Inspection of the mesh under the microscope shows small areas with irregular construction of the Nylon matrix (see Figure E.1.).

Detailed measurements were taken using the same microphotograph of Figure E.1. but from other larger areas of it, and also using lengths measurements based in the standard obtained equivalent to: 134 pixels = 100 µm. We obtained 16 measurements at ramdom locations giving an average pore area of: 74.7 µm², with pores as large as 137 µm² and as small as 24.5 µm².

We were able to see that the pores were not round but rectangle and square shaped of different sizes. We need to concider that for *Dunaliella* cells passing through the mesh facing the mesh by its length, for example 10 µm, the pore at least should be 78.5 µm² if we think in a round pore. If the cell faces the mesh by its width, for example 5 µm, the pore should be at least 19.6 µm², also thinking in a round pore. Besides this last observation, we obtained an average mesh pore density of 11 pores/ 49218.6 µm². The microchamber outlet is 1,9 mm in diameter and the mesh is mounted here, covering an area of 2835287 µm² with 633 pores inside of it.

This simple observation gave a strong support to the mesh irregular size porosity hypotheses, as a cause of the mesh low cell retention capacity of 36.3%

Reynolds numbers associated with flow at different rates are summarized in Table 4.1 and these confirmed that culture media flow inside the microreactor was laminar. Future designs would require an agitation system to overcome the lack of mixing and the ineffective agitation provided by incoming flow at the bottom of the microchamber. Increasing fluid velocity to increase Re in this case might not be practical since the turbulent flow needed for good agitation also will increase hydrodynamic forces that can give rise to cell damage. Adding more inlets might solve the problem to an extent, but the fundamental flow regime will remain laminar. Also, agitation is based on the influx of culture medium and some tests may not require medium replacement or circulation. An alternative independent agitation system would be an important addition to this design.

5.5 Surface Retention

Internal surfaces of the microchannels and structures created with 3D printer used in this work have a high degree of rugosity that can be problematic since processes such as disinfection, and flushing of debris, cells and other remaining material become difficult when the surface contributes to the retention of microscopic material.

The surface rugosity is likely to result from a combination of the support material and the characteristic and intrinsic material additive technique used in 3D printing. A support material extraction method that is effective in regions such as microchannels and internal walls, and that can be carried out with minimal mechanical deformation of the polymer material, is desired. In the present study this method was not ideal. Cells were present in areas surrounded and protected by polymer material, making their removal

difficult. In Figure 4.7, images B and D were acquired from the inlet area, and this area was highly accessible to water jet cleaning, therefore most of the support material should have been removed. On the microchannel internal surface, image 4.7 C, the adherence of debris on the internal walls suggests that residual support material remained even though it should have been flushed out using the high pressure water jet. A new support material chemical extraction method or the elimination of support material from the fabrication of microchannels or enclosed microstructures in the 3D printing process should be considered.

5.6 Optical measurement and methods for promoting algal stress

5.6.1 Light scattering measurement and microscopy

Cell density in the microchamber was measured by detection of scattered light with a photosensor held at 90 degrees to the incident illumination with 515 nm green light. The intensity of light reaching the photodetector should have been proportional to cell concentration. The light impinging on the photodetector was detected and the signal transformed to a square wave signal with a frequency proportional to light intensity. The obtained values of frequency, maximum and minimum testing different cell concentrations were in a 0.95 Hz range. The measurement of scattered light was not straightforward, since unwanted light coming either from reflection on the glass slide or from light leakage at the photosensor window touching the glass slidem which masked the weak signal from the scattered beam. A collimator lens was used to focus the

divergent light beam from the RGB LED into the chamber, improving photodetection efficiency, which was necessary for reading light scattering by the microalgal cells.

Even with this improvement in light intensity reading, it was not sufficient to provide a broader range reading. The gap between the photosensor window and the glass slide helped in bringing light from unwanted sources and for solving this, black rubber was positioned around the photosensor, sealing the gap with the glass slide and avoiding this external unwanted light. Photosensor resolution was once again increased in some degree.

Fiber optics were not tested for conducting light to the scattered light sensors. Circular channel for passing this fiber to the microchamber was successfully created.

The bottom window was also used for microscopy observation and allowed inspection and counting of microalgae using a standarized image frame-based system as a backup method for the scattering-based cell density measurement. Both techniques accurately measured cell density. Since microalgal growth could not be maintained over a period of time sufficient to allow measurable changes in cell density measurable by light scattering the automatic cell density measuring system was not tested over the entire several day growing period.

5.6.2 Light irradiance for stress induction

The culture system was designed to produce stress in *Dunalliela sp* by exposure to high light irradiance, as well as by salinity increase, resulting in stimulation of carotenoid production. Ideally the stressing light photon flux density is in the range of 200-1200 µE

$m^{-2}s^{-1}$ (47.4 Wm^{-2}- 284.6 Wm^{-2} , PAR correlation) for carotenoid production [19]. In the present system the maximum photon flux reached when using the RGB LED was 115 µE $m^{-2}s^{-1}$ (27.28 Wm^{-2}, PAR correlation) inside the microchamber. When a photon flux meter sensor touched the RGB LED epoxy lens, values as high as 1084 µE $m^{-2}s^{-1}$ (257.14 Wm^{-2}, PAR correlation) were measured but in the case of the microdevice, the RGB LED light had to travel through the focal length f = 9.85 mm and a collimator lens, used as a window in the chamber, until it reached the microalgae with a value of 115 µE $m^{-2}s^{-1}$ (27.28 Wm^{-2}, PAR correlation). In the macro experiment with flask cultures light intensities of 380 µmol $m^{-2}s^{-1}$ (90.14 Wm^{-2}, PAR correlation) were achieved as a light stressing condition. Other factors that contributed to the reduction in photon flux in the microreactor was the decrease in diameter of the window through which light passed into the microchamber. In this case the RGB LED was 5 mm in diameter and the microchamber window, where the lens is mounted, was 3.46 mm in diameter.

To increase the efficacy of stressing light, a 375 nm UV LED was mounted facing the RGB LED from the opposite side of the microchamber. This LED worked well from a functional and control point of view but its ability to produce a stress response in *Dunaliella sp* was not tested because of problems with culture growth and stability over time. In general it can be seen that use of light for stress factor is a challenge if high photon flux levels, in the range of 200-1200 µE $m^{-2}s^{-1}$ (47.4 Wm^{-2}- 284.6 Wm^{-2} , PAR correlation), are desired in small areas and volumes. Fiber optics were considered as a conduit for stress-inducing illumination but photon fluxes achieved without a collimator lens, using the RGB LED as the source of light for the fiber, were in the range of 12 µE

$m^{-2}s^{-1}$ (2.84 Wm^{-2} PAR correlation) which was far below the intensity required to stress *Dunalliela sp*.

5.7 Specific growth rate and microreactor environment parameters

Specific growth rate was not determined in the microreactor environment because stable reproduction of microalgae was not achieved. Different hypotheses may be proposed to explain the failure of the microalgae to reproduce in the microdevice. Microalgae growth tests used red and blue light with a photon flux density together of 40 µE $m^{-2}s^{-1}$ (9.48 Wm^{-2}, PAR correlation) , reaching 27 °C because of the heat produced by the RGB LED.

Dunaliella tertiolecta has been grown effectively in the range of 12 to 28 °C [28]. The salinity was adjusted to 31 ppt and 48 ppt in different experiments to determine whether this influences the growth rate decline but no data supporting this was found.

CO_2 was added to new culture medium by constant aeration of a new media flask through a sterile 0.45 µm filter.

Microalgae grew well in flasks (macro culture) using CO_2 in air, in this case the flask is always receiving a new dose of CO_2 through the air pump, but it is not clear that it was enough CO_2 for the microreactor culture since pumping syringe was loaded with culture media once (media originally coming from the aerated flask) and no additional CO_2 was added to this media. At the end, the CO_2 received by the microreactor had to come from the one contained inside the syringe.

No direct dissolved concentration reading inside the microchamber was available. As mentioned in 5.3, poor agitation played an important role in gas and nutrient transport to the cells, which could have been a contributing factor in the absence of cell replication. By microscopy it was possible to see cells moving away from the incoming media inlet at the bottom of the chamber close to the glass slide window, but this flow did not mix the entire microchamber, i.e. cells at not exposed to mixing did not move, and so did not encounter a better exchange of nutrients and necessary gases.

Among the 3 culture trials in Figure 4.9 , the one at 31 ppt which reached 200000 cell ml^{-1} at day 2 (green line), is the only trial in which the culture medium had a pH under 7 (6.88) and this was product of a direct small dose of pure CO_2 injection in the culture media flask before pumping into the microchamber. This direct injection of CO_2 was performed to stimulate cell replication in the culture and to determine whether the lack of CO_2 was a reason for poor growth in the cell population. Buffer solutions were never added to the culture media. Direct injection of CO_2 into the culture media in future experiments will require the addition of a pH buffer to avoid a dramatic decreases in pH.

Theoretical concentration of CO_2 inside the microchamber sea water media was calculated. In the experiment for microalgae growth rate inside the microreactor, the CO_2 came from a syringe loaded with fresh seawater media and nutrients. This CO_2 and fresh new media came from a flask fed with air and the flask had a ventilation to atmosphere . The application of Henry´s Law in this case would be at 1 atm (1.0132 bar).

According to previous reports of *Dunaliella tertiolecta* semi continuos culture [50] we have considered a value of CO_2 consumption rate = 110 mg L^{-1} d^{-1} (0.00127 mg L^{-1} sec^{-1}). For CO_2 solubility in sea water we have taken in consideration the table from Al-Anezi et al [49] (see Apendix H). This table gives a value for Henry´s Law coefficient = 29.3 mol m^{-3} bar^{-1} (25 ˚C, S = 35 ppt, CO_2 partial pressure = 0.0003 bar (note that with rising CO2 in the atmosphere, the partial pressure may be closer to 0.0004) resulting a concentration of CO_2 = 0.4 mg Kg^{-1} (sea water). Using density of seawater = 1023.37 Kg m^{-3} (25 ˚C, S = 35 ppt) and the volume of microchamber we obtained 0.00003 mg CO_2/ 70.33 µL (0.426 mg L^{-1}).

From this point we can see that 0.426 mg L^{-1} / 0.00127 mg L^{-1} sec^{-1} (consumption rate) gives us a value equivalent to 5.59 minutes. This last value is a strong support for the CO_2 deficiency as a leading cause for microalgae growth failure, since at that rate of CO_2 consumption it would have been necessary to pump 70.33 µL of new media each 5.59 minutes. In the real experiment the highest dose of new media/day was 70 µL and from here is easy to see the CO_2 depletion problem.

Polymer material used by the 3D printer for building the last prototype (Vero™ Black) is labeled, according to the manufacturer, as intermediate (better) according to a 3 level classification (good, better and best) with respect to biocompatibility.

Even with this ´´better´´ classification of the polymer, the sensitivity of cells to this material is unknown from this work and if this material has effects on the normal growth of microalgae is also unknown.

Some information included in a recent work [29], shows that Vero Clear (almost the same polymer material used in our experiment, except without pigmentation) was used in a 3D printed microfluidic device and is reported that the material "*supports adhesion and growth of endothelial cells, but incorporation of cells into a fluidic channel yielded minimal cell adherence and poor viability over a 24 h period* ". Further work must be carried out to characterize any possible effects of Vero Black 3D polymer material on microalgae growth and if the material was a contributing factor to the failure of the microalgae to replicate.

Most proprietary resins for use with commercial 3D-printers have not been assessed for their biosafety and biofunctionality at this writing [39]. For future work, we note that good biocompatibility potential candidates for 3D printing have been used for myocyte encapsulation, like hydrogel matrices made with polyethylene-glycol-diacrylate [40][41], poly-ethylene-glycoldimethacrylate[42], gelatin methacrylate [43][44], hyaluronic acid [45] and functionalized methacrylic alginates [46].

One of the disadvantages of using the type of 3D printing polymer in this work, compared to the very well known PDMS, is that the photopolymer used here does not diffuse gases like CO_2, N_2, O_2 in the same way as PDMS which permits diffusion of these gases without major problems at different permeability coefficients according to the gas nature. This is a disadvantage for the photopolymer in comparison to PDMS since for example, we needed to find other way to supply CO_2 to the microalage inside the microchamber.

A possible future solution for this would be the integration of PDMS into a hybrid structure composed of 3D printing polymer as the base material and exposing part of the PDMS surface directly to the microculture chamber as a gas transfer layer, allowing good CO_2 exchange, for example. Part of the challenge here would be the tight bonding between PDMS and the 3D printer polymer.

Loctite® Clear Silicone waterproof sealant was used for sealing microchamber bottom window with the glass slide and also for sealing the micromesh at the microreactor top outlet when part A and B were assembled. This type of sealant uses an acetoxy tin condensation reaction for curing silicone at room temperature. This process produces acetic acid during curing, which should have been removed when the reactor went through the cleaning and disinfection process, before the reactor was used. This point needs to be addressed in future work to minimize any possible effects of the acid on the cells.

CHAPTER 6

CONCLUSIONS

We explored the use of a commercially available 3D printer for the fabrication of a microbioreactor for microalgal culture and testing. The microbioreactor device was successfully built using the additive manufacturing technique with an Objet 30 Pro (Stratasys, Polyjet Technology USA-Israel) employing jetted UV-cured photopolymer. The microbioreactor device was 40 mm X 21.9 mm X 19,03 mm (width × depth × height) and contained a microchannel network for culture media and cell inoculum flow, a microculture chamber for microalgal growth and stress testing, and a semi-integrated photodetection system for measuring optical density and intrinsic fluorescence of microalgal cultures.

Forty five g of photopolymer material were used, at a cost of 0.90 US$/g and 17 g of support material at a cost of 0.40 US$/g. Fabrication time was 1 hour and 49 minutes.

From an economic point of view, and putting aside photopolymer and support material costs mentioned before, the microbioreactor was built with a 3D printer that has an average market cost of $US 20,000 and this can not be considered inexpensive if other milli-microfluidic devices have been reported to have been built with 3D printers in the range of $US 2,000 [9], but this cost can be relative if the 3D printing equipment not necessarily belong to a unique department in a production facility and it is shared with other processes.

The microculture chamber itself was not able to maintain a growing population of microalgal cells, and the cause of this finding still unknown. Several hypotheses may explain the lack of growth. One of the strongest hypotheses predicts that the low content of CO_2 in the culture medium and inside the culture chamber limited algal growth.

The CO_2 hipotheses was supported also by calculation of CO_2 solubility in the microchamber, equivalent to 0.426 mg L^{-1} and that would last for only 5.59 minutes inside the microchamber for an average *Dunaliella tertiolecta* CO_2 consumption rate.

Another related problem could have been insufficient agitation from medium entering from the bottom of the microchamber, which did not allow ideal distribution of nutrients and gases. PDMS may provide advantages when compared with the photopolymer material used in this work, particularly with respect to gas exchange.

Potentially, work in hybrid systems containing a mix of PDMS and photopolymer structures might help solve gas exchange problems.

Device assembly of photopolymer structures, is relatively simple, but inclusion of external components such as microlens for light collimation, a bottom glass slide, micromesh and reactor windows add a significant amount of complexity to the fabrication process that extends well beyond the 3D printing process. Internal microchannels and microchamber surfaces show unwanted cell retention, rendering them less than ideal for disinfection and device reuse.

The use of support material in enclosed structures like microchannels complicates the cleaning process and an alternative method such as 3D printing without support material, might be very beneficial for future work.

The microalgae retention system was 36.3% effective, therefore a better system for avoiding escape of microalgae from microchamber in continuous culture needs to be addressed in any future work, considering the observations that support the mesh irregular size porosity hypotheses, as a cause of the mesh low cell retention capacity of 36.3%.

Semi-integration of the optical measuring system and light control was possible, but further tests of the measuring system in continues microalgae growing cycles need to be done. Irradiances in the range of 380 $\mu E/m^2s$ (90.14 Wm^{-2}, PAR correlation), the intensity used in the flask stress experiment, was impossible to obtain in the microchambers using the RGB LED in the present microreactor configuration. Alternative methods to increase stressing light irradiance in the range of 1000 $\mu E/m^2s$ (237.2 Wm^{-2}, PAR correlation) for optimal carotenoid production biotests are required. Any increase in irradiance needs to take in account the increase of heat in the microbioreactor and the way to control the normal temperature range for the microorganism.

3D printing offers great potential in the development of microfluidics applications. Development of new 3D printed photoplymer materials that may have some properties similar to PDMS in the gas exchange aspect or a biomechanical or biochemical resemblance with natural biological enviroments like the ones found in specific cellular

tissues can help in the application of 3D printing techniques to create microenvironments for cell and microorganism tests.

According to initial thesis statement: *A micro-milli fluidic bioreactor can be fabricated using simple, rapid, inexpensive and reliable additive manufacturing (3D printing), and that this device can be used to study microalgal growth and biosynthesis*, It can be stated that further improvements are required and since no demonstration of microalgal growth and biosynthesis was achieved, the statement has not been demonstrated completely and future work must address the observations related to a lack of cell replication in the microreactor.

From a purely mechanical point of view, it is possible to build the milli-microfluidic bioreactor rapidly, simply and reliably using 3D printing and this was demonstrated in this work. The initial investment cost is high in this case, compared to other 3D printers in the market, but the manufacturing process cost is still relatively low compared with labor, specialized personnel, equipment, time, and energy used invested in other microfabrication processes. Finally, it is evident that the reduction of culture media, materials, equipment and labor in tests for microalgae may be reduced substantially by using a microbioreactor with microalgal tests in flask cultures.

REFERENCES

1. Hegab, Hanaa M.;ElMekawy, Ahmed and Stakenborg,Tim. Review of microfluidic microbioreactor technology for high-throughput submerged microbiological cultivation. Biomicrofluidics., 2013, 7, 021052.

2. Pasirayi,Godfrey.; Auger,Vincent.; Scott, Simon M.; Rahman, Pattanathu K.S.M.; Islam,Meez.; O'Hare,Liam.; Ali, Zulfiqur. Microfluidic Bioreactors for Cell Culturing: A Review. Micro and Nanosystems., 2011,3,137-160

3. Nagel,B.; Dellweg, H.; Gierasch, L. M. Glossary for chemists of terms used in biotechnology (IUPAC Recommendations 1992).Pure and Applied Chemistry., 1992, Volume 64, Issue 1, Pages 143–168, ISSN (Print) 0033-4545

4. Xia, Y.; Whitesides, G. M. Soft lithography. Annu. Rev. Mater.,1998, 28, (1), 153-184.

5. Schift, H.; David, C.; Gobrecht, J.; D'Amore, A.; Simoneta, D.; Kaiser, W.; Gabriel, M. Quantitative analysis of the molding of nanostructures. J Vac Sci Technol B., 2000, 18, (6), 3564-3568.

6. Attia, U. M.; Marson, S.; Alcock, J. R. Micro-injection moulding of polymer microfluidic devices. Microfluid Nanofluid., 2009, 7, (1), 1-28.

7. Comina,German.; Suska,Anke.; Filippini,Daniel. PDMS lab-on-a-chip fabrication using 3D printed templates. Lab on a Chip., 2013, DOI:10.1039/C3LC50956G.

8. Kitson, Philip J.; Rosnes, Mali H.; Sans, Victor.; Dragone, Vincenza.; Cronin, Leroy. Configurable 3D-Printed millifluidic and microfluidic 'lab on a chip' reactionware devices. Lab Chip., 2012, 12, 3267–3271.

9. Shallan, Aliaa I.; Smejkal, Petr.; Corban, Monika.; Guijt, Rosanne M.; Breadmore, Michael C. Cost-Effective Three-Dimensional Printing of Visibly Transparent Microchips within Minutes. Analytical Chemestry., 2014, 86, 3124−3130.

10. Isabelle, Walther. Space Bioreactors and their Applications. Space Biology Group ETH-Technopark. Cell Biology and Biotechnology in Space., 2012

11. Wonjae, Lee.; Donghoon, Kwon.; Woong, Choi.; Gyoo,Yeol Jung.; Sangmin, Jeon. 3D-Printed Microfluidic Device for the Detection of Pathogenic Bacteria Using Size-based Separation in Helical Channel with Trapezoid Cross-Section. Scientific Reports., 2014, 5, 7717 doi:10.1038/srep07717.

12. Betts,I.;Baganz,F.Miniature bioreactors: current practices and future opportunities. Microbial Cell Factories., 2006, 5:21 doi:10.1186/1475-2859-5-21.

13. Zimmerman,William B.J . Microfluidics: History, Theory and Applications. CISM courses and lectures. International Centre for Mechanical Sciences., 2006, 466.

14. Figallo, E.; Cannizzaro, C.; Geretcht, S.; Burdick, J.A.; Langer,R.; Elvassore, N.; Vunjak-Novakovic, G. Micro-bioreactor array for controlling cellular microenvironments. Lab Chip., 2007, 7, (6), 710-719.

15. Freshney, I.; Obradovic, B.; Grayson, W.; Cannizzaro, C.; VunjakNovakovic, G. In: Principles of Tissue Engineering; R. Lanza, R. Langer, R.; Vacanti, J. Eds.; Academic Press: USA,2007; pp. 55– 184.

16. Au, Anthony.; Bhattacharjee, Nirveek; Horowitz, Lisa.; Chang, Tim.; Folch, Albert. 3D-printed microfluidic automation. Lab Chip., 2015,15, 1934-1941.

17. Richmond, Amos. Handbook of microalgal culture: biotechnology and applied phycology., 2004, ISBN-10:0-632-05953-2.

18. Oren, A. 2005. A hundred years of Dunaliella research: 1905-2005. Saline Systems. 1:2

19. Guedes, A.; Amaro, Helena.;Malcata, Xavier. Microalgae as Sources of Carotenoids. Marine Drugs., 2011, 9, 625-644; doi:10.3390/md9040625, ISSN 1660-3397

20. Lichtenthaler, H.K. Chlorophylls and carotenoids: pigments of photosynthetic biomembranes. Methods Enzymol., 1987, 148, 350-382.

21. Fazeli, Mohammad.R; Tofighi, Hossein, Samadi, Nasrin; Jamalifar, Hossein; Fazeli, Ahmad. Carotenoids accumulation by *Dunaliella tertiolecta* (Lake Urmia isolate) and *Dunaliella salina* under stress conditions. Tehran University of Medical Sciences. DARU., 2006, Volume 14, No.3.

22. Borowitzka, LJ.; Borowitzka, MA.; Moulton, T. 1984. Mass culture of *Dunaliella*: from laboratory to pilot plant. Hydrobiologia., 1984, 116/117:115–121.

23. Chakraborty, Suman. Microfluidics and Microfabrication. Department of Mechanical Engineering. Indian Institute of Technology. India ISBN 978-1-4419-1542-9/e-ISBN 978-1-4419-1543-6 DOI 10.1007/978-1-4419-1543-6.

24. Ruan, J.; Wang, L.; Xu, M.; Cui, D.; Zhou, X.; Liu, D. Fabrication of a microfluidic chip containing dam, weirs and gradient generator for studying cellular response to chemical modulation. Mater Sci Eng:C.,2009, 29, (3), 674-679.

25. Weibel,D. B.;Whitesides, G. M. Applications of microfluidics in chemical biology. Curr. Opin. Chem. Biol.,2006,10, (6),584-591.

26. (a) Illg, T.; Lob, P.; Hessel, V. Bioorg. Med. Chem., 2010, 18, 3707–3719; (b) Li, Y.; Sanampudi, A.; Reddy, V. Raji.; Biswas, S.; Nandakumar, K.; Yemane, D.; Goettert, J. and C. S. S. R. Kumar, ChemPhysChem, 2012, 13, 177–182.

27. Waldbaur,A.; Rapp,H.;Lange,K. and Rapp, B. E. Anal. Methods, 2011, 3, 2681–2716.

28. Sosik, Heidi.; Mitchell, B.Greg. Effects of temperature on Growth, light Absorption, and Quantum Yield in *Dunaliella Tertiolecta* (Chlorophycea)1. Journal of Phycology., 1994, Volume 30, Issue 5, 833–840.

29. Gross, Bethany C.; Anderson, Kari B.; Meisel, Jayda E.; McNitt, Megan I.; and Spence, Dana M. Polymer Coatings in 3D-Printed Fluidic Device Channels for Improved Cellular Adherence Prior to Electrical Lysis DOI: 10.1021/acs.analchem.5b01202 Anal. Chem. 2015, 87, 6335−6341

30. Bourbeau, PP.; Ledeboer, NA. Automation in clinical microbiology. J Clin Microbiol. 2013; 51: 1658-1665.

31. Greub, G.; Prod'hom, G. Automation in clinical bacteriology: what system to choose? Clin Microbiol Infect. 2011; 17: 655-660.

32. Mutters,Nico.T.Laboratory Automation in Clinical Microbiology: A Quiet Revolution. Department of Infectious Diseases. Heidelberg University Hospital, Germany, Department of Infectious Diseases, Heidelberg University Hospital. Im Neuenheimer Feld 324, D-69120 Heidelberg, Germany, Published: April 08, 2014.

33. Shuler, Michael.L; Kargi,Fikret. Bioprocess Engineering Basic Concepts. Prentice Hall College Div., 2nd Ed., 2002. ISBN: 9780130819086.

34. Vyawahare, S.; Griffiths, A. D.; Merten, C. A. Miniaturization and parallelization of biological and chemical assays in microfluidic devices. Chem Biol., 2010, 17, (10), 1052-1065.

35. Pick, U. 2002. Adaptation of the halotolerant alga Dunaliella to high salinity. In A Lauchli, Luthge, (eds), Salinity: Enviroment, Plants, Molecules. Kluwer Academic Publishers, Dordrecht, the Netherlands, 97-112.

36. Kleinegris, Dorinde M. M.; van Es, Marjon A.; Janssen, Marcel.; Brandenburg, Willem A.; Wijffels, René H. Carotenoid fluorescence in *Dunaliella salina.* J Appl Phycol (2010) 22:645–649 DOI 10.1007/s10811-010-9505-y

37. Subramaniyan Venkatesan; Munuswamy Senthil Swamy; Chinnasamy Senthil; Sailendra Bhaskar and Ramasamy Rengasamy. Culturing Marine Green Microalgae Dunaliella salina Teod. and Dunaliella tertiolecta Masjuk in Dewalne's Medium for Valuable Feeds Stock. Journal of Modern Biotechnology, Volume 2, Number 2, March 2013.

38. Gillbro, T.; Cogdell, RJ. (1989) Carotenoid fluorescence. Chem Phys Lett 158:312–316.

39. Bhattacharjee, Nirveek.; Urrios, Arturo.; Kang,Shawn.; Folch, Albert. The upcoming 3D-printing revolution in microfluidics. Lab Chip, 2016,16, 1720

40. Chan, V.; Zorlutuna, P.; Jeong, J. H.; Kong, H.; Bashir, R. Lab Chip, 2010, 10, 2062–2070.

41. Han, L.-H.; Suri, S.; Schmidt, C. E.; and Chen, S. Biomed. Microdevices, 2010, 12, 721–725.

42. Mapili, G.; Lu, Y.; Chen, S.; Roy, K. J. Biomed. Mater. Res., Part B, 2005, 75, 414–424.

43. Grogan, S. P.; Chung, P. H.; Soman, P.; Chen, P. ; Lotz, M. K.; Chen, S.; D'Lima, D. D. Acta Biomater., 2013, 9, 7218 –7226.

44. Soman, P.; Chung, P. H.; Zhang, A. P.; Chen, S. Biotechnol. Bioeng., 2013, 110, 3038–3047.

45. Suri, S.; Han, L.-H.; Zhang, W.; Singh, A.; Chen, S.; Schmidt, C. E. Biomed. Microdevices, 2011, 13, 983–993.

46. Zorlutuna, P.; Jeong, J. H.; Kong, H.; Bashir, R.; Adv. Funct. Mater. 2011, 21, 3642–3651.

47. Tafreshi, A. Hosseini.; Shariati, M. *Dunaliella* biotechnology: methods and applications. Journal of Applied Microbiology., 107 (2009) 14–35.

48. Ahmad,Parvaiz. Oxidative Damage to Plants. Antioxidant Networks and Signaling. 2014, 9, 289-295.

49. Al-Anezi,Khalid.;Hilal,Nidal. Effect of Carbon Dioxide in Seawater on Desalination: A Comprehensive Review, Separation & Purification Reviews.2006, 35:3, 223-247, DOI: 10.1080/15422110600867365.

50 Farrelly, Damien J.; Brennan, Liam.; Everard,Colm D.; McDonnell, Kevin P. Carbon dioxide utilisation of Dunaliella tertiolectafor carbon bio-mitigation in a semicontinuous photobioreactor. Appl Microbiol Biotechnol.2014, 98: 3157. doi:10.1007/s00253-013-5322-y.

APPENDIX A: MICROREACTOR SPECIFIC GROWTH RATE TESTS DATA

Table A.1 Microreactor Specific Growth Rate Test Data
Microalgae: *Dunaliella tertiolecta*

Date	Day	Temp C°	Salinity ppt	Light Irradiance µE m⁻¹ s⁻¹ /Photoperiod ()D: Hours day ()N:Hours Night RB: Red Blue Light	Microscope cell counting (20X Objective) Camera frame area: 251313 µm²	cell mL⁻¹ equivalency from frame area and calibration curve	cells/chamber (70.33 µL)	cells µL⁻¹	Media Flow µL min⁻¹	Media Dose times/ day	Total Media Dose µL	% Media Exchange	CO_2 mg L⁻¹	O_2 mg L⁻¹	pH media	pH inoculum	Note
MICRO 4	EXPERIMENT																
7/17/2015	0	23.3	31	33 18D/6N RB	-	238201	16753	238	5	-	7	-	-	4.3	7.77	-	
7/18/2015	1	23.3	31	33 18D/6N RB	-	238201	16753	238	5	-	74.3	-	-	-	-	-	Not Growing
7/19/2015	2	23.3	31	33 18D/6N RB	-	238201	16753	238	5	-	0	-	-	-	-	-	
MICRO 5	EXPERIMENT																
7/19/2015	0	27	48	40 18D/6N RB	34	808306	56892	809	5	1	70	100	2	4.3	7.77	7.67	Declining
7/20/2015	1	27	48	40 18D/6N RB	34	808306	56892	809	5	1	40	57	-	-	-	-	cell population
7/21/2015	2	27	48	40 18D/6N RB	0.33	150384	10577	150	5	1	40	57	-	-	-	-	Figure 4.10
7/22/2015	3	27	48	40 18D/6N RB	0.33	150384	10577	150	5	1	40	57	-	-	-	-	
7/23/2015	4	27	48	40 18D/6N RB	0.1	145886	10260	146	5	1	40	57	-	-	-	-	
MICRO 6	EXPERIMENT																
7/23/2015	0	27	31	40 18D/6N RB	34	808306	56892	809	10	1	70	100	0	5.9	8.53	7.67	Declining
7/24/2015	1	27	31	40 18D/6N RB	34	808306	56892	809	20	1	10	14	0	5.9	8.1	7.67	cell population
7/25/2015	2	27	31	40 18D/6N RB	30	730700	51390	731	35	1	20	28	0	5.9	8.1	7.67	Figure 4.10
7/26/2015	3	27	31	40 18D/6N RB	30	730700	51390	731	50	1	40	57	0	5.9	8.1	7.67	
7/27/2015	4	27	31	40 18D/6N RB	0	1433930	10123	144	50	1	40	57	0	5.9	8.1	7.67	
MICRO 7	EXPERIMENT																
7/29/2015	0	27	32	40 18D/6N RB	-	-	-	-	-	-	-	-	-	-	-	-	Injection of CO_2+Bicarbonate
7/30/2015	1	27	32	40 18D/6N RB	-	-	238201	16753	238	5	1	110	156	39	4.4	8.34	low pH, not growing
7/31/2015	2	27	33	40 18D/6N RB	-	-	238201	16753	238	5	1	-	0	13	4.4	8.57	Rounded cells shape
8/1/2015	3	27	33	40 18D/6N RB	-	-	238201	16753	238	5	1	-	0	13	4.4	8.57	Bubble inside chamber, stopped
MICRO 8	EXPERIMENT																
8/3/2015	0	27	31	40 18D/6N RB	11	353079	25254	353	10	1	-	0	0	0	-	-	Declining
8/4/2015	1	27	31	40 18D/6N RB	3	202607	14243	203	10	1	10	14	10	4.6	6.88	-	cell population
8/5/2015	2	27	31	40 18D/6N RB	3	202607	14243	203	10	1	50	71	10	-	-	-	Figure 4.10

APPENDIX B: MACRO CULTURE TESTS (FLASK) DATA

Table B.1 Macro (flasks) Specific Growth Rate Test
Microalgae: *Dunaliella tertiolecta*

Date	Day	Temp C°	Salinity ppt	Light Irradiance µE m^{-2} s^{-1} /Photoperiod ()D: Hours day () N:Hours Night	Culture Time (Hours)	Haemocytometer count	Cell mL^{-1}	Culture Volume (mL)
FLASK 1								
5/16/2015	0	21.6	35	60-18D/6N	0	0.89	222500	250
5/17/2015	1	21.6	35	60-18D/6N	24	0.89	222500	250
5/18/2015	2	21.6	35	60-18D/6N	48	1.2	300000	250
5/19/2015	3	21.6	35	60-18D/6N	72	1.2	300000	250
5/20/2015	4	21.6	35	60-18D/6N	96	1.9	475000	250
5/21/2015	5	21.6	35	60-18D/6N	120	1.9	475000	250
5/22/2015	6	21.6	35	60-18D/6N	144	4.1	1025000	250
5/23/2015	7	21.6	35	60-18D/6N	168	4.1	1025000	250
5/24/2015	8	21.6	35	60-18D/6N	192	7.1	1775000	250
5/25/2015	9	21.6	35	60-18D/6N	216	7.1	1775000	250
FLASK 2								
5/16/2015	0	21.6	35	60-18D/6N	0	0.75	187500	250
5/17/2015	1	21.6	35	60-18D/6N	24	0.75	187500	250
5/18/2015	2	21.6	35	60-18D/6N	48	1.18	295000	250
5/19/2015	3	21.6	35	60-18D/6N	72	1.18	295000	250
5/20/2015	4	21.6	35	60-18D/6N	96	3	750000	250
5/21/2015	5	21.6	35	60-18D/6N	120	3	750000	250
5/22/2015	6	21.6	35	60-18D/6N	144	5.09	1272500	250
5/23/2015	7	21.6	35	60-18D/6N	168	5.09	1272500	250
5/24/2015	8	21.6	35	60-18D/6N	192	6.5	1625000	250
5/25/2015	9	21.6	35	60-18D/6N	216	6.5	1625000	250
FLASK 3								
5/16/2015	0	21.6	35	60-18D/6N	0	0.75	187500	250
5/17/2015	1	21.6	35	60-18D/6N	24	0.75	187500	250
5/18/2015	2	21.6	35	60-18D/6N	48	1.31	327500	250
5/19/2015	3	21.6	35	60-18D/6N	72	1.31	327500	250
5/20/2015	4	21.6	35	60-18D/6N	96	2.4	600000	250
5/21/2015	5	21.6	35	60-18D/6N	120	2.4	600000	250
5/22/2015	6	21.6	35	60-18D/6N	144	4.45	1112500	250
5/23/2015	7	21.6	35	60-18D/6N	168	4.45	1112500	250
5/24/2015	8	21.6	35	60-18D/6N	192	5.6	1400000	250
5/25/2015	9	21.6	35	60-18D/6N	216	5.6	1400000	250

Date	Day	Culture Time (Hours)	Cell mL^{-1}	Specific Growth Rate Day 2-8 (µ)	Doubling Time
Flask 1-2-3 Arithmetic mean					
5/16/2015	0	0	199167	0.01	60.5
5/17/2015	1	24	199167		
5/18/2015	2	48	307500		
5/19/2015	3	72	307500		
5/20/2015	4	96	608333		
5/21/2015	5	120	608333		
5/22/2015	6	144	1136667		
5/23/2015	7	168	1136667		
5/24/2015	8	192	1600000		
5/25/2015	9	216	1600000		

APPENDIX C: PHOTOSENSOR AND MICROSCOPY AREA CALIBRATION

Table C.1 Photosensor and Microscopy Area Calibration.

Inoculum cell mL^{-1}	Microscope cell counting (20X Objective) Camera frame a 251313 μm^2	TAOS sensor frecuency (Hz) Green filter (524 n 525 nm LED	Oscilloscope setting msec	Relative Intensity
0 (space)		5.54	100.00	0.00
0	0.00	6.50	100.00	0.00
363636	13.00	6.55	100.00	0.06
636363	22.00	-	100.00	0.06
1068181	37.00	-	100.00	0.06
1996000	99.00	7.45	100.00	1.00
2527777		6.78	100.00	0.29

APPENDIX D: CAROTENOIDS PRODUCTION UNDER STRESS IN MACRO TESTS (FLASKS) CULTURE (*Dunaliella salina*).

Table D.1 Carotenoids Production under Stress. in Macro Tests (Flasks), Microalgae: *Dunaliella salina*

Date	Day	Temp C°	Salinity ppt	Light Irradiance µE m^{-2} s^{-1} 24 hours/day Light	Haemocytometer count	Cell mL^{-1}	Culture Volume (mL)	pH Culture
Flask S1								
6/7/2015	0	23	120	380	1.25	304166	250	7.7
6/8/2015	1	23	120	380		0	250	7.7
6/9/2015	2	23	120	380		0	250	7.7
6/10/2015	3	23	120	380		0	250	7.7
6/11/2015	4	23	120	380		0	250	7.7
6/12/2015	5	23	120	380		0	250	7.7
6/13/2015	6	23	120	380		0	250	7.7
6/14/2015	7	23	120	380	9	2250000	250	7.7
Flask S2								
6/7/2015	0	23	170	380	1.3	304166	250	7.7
6/8/2015	1	23	170	380		0	250	7.7
6/9/2015	2	23	170	380		0	250	7.7
6/10/2015	3	23	170	380		0	250	7.7
6/11/2015	4	23	170	380		0	250	7.7
6/12/2015	5	23	170	380		0	250	7.7
6/13/2015	6	23	170	380		0	250	7.7
6/14/2015	7	23	170	380	4.5	1125000	250	7.7
Flask S3								
6/7/2015	0	23	220	380	1.1	304166	250	7.7
6/8/2015	1	23	220	380		0	250	7.7
6/9/2015	2	23	220	380		0	250	7.7
6/10/2015	3	23	220	380		0	250	7.7
6/11/2015	4	23	220	380		0	250	7.7
6/12/2015	5	23	220	380		0	250	7.7
6/13/2015	6	23	220	380		0	250	7.7
6/14/2015	7	23	220	380	2.77	692500	250	7.7

Table D.2 Carotenoids Extraction (Before and After Stress) in Macro Tests (Flasks), Microalgae: *Dunaliella salina*

Initial Carotenoids Extraction						
	Flask 1		Flask 2		Flask 3	
Absorbance Readings	663.2	0.26	663.2	0.16	663.2	0.19
(At wave length)	646.8	0.12	646.8	0.07	646.8	0.09
	470	0.32	470	0.21	470	0.24
Calculation	Ca	2.88	Ca	1.81	Ca	2.09
	Cb	1.14	Cb	0.67	Cb	0.92
	Ca+b	4.02	Ca+b	2.48	Ca+b	3.01
Carotenoids (µg/mL extract)	Cx+c	0.74	Cx+c	0.75	Cx+c	0.79
Final Carotenoids Extraction						
Absorbance Readings	663.2	0.25	663.2	0.23	663.2	0.28
(At wave length)	646.8	0.08	646.8	0.09	646.8	0.11
	470	0.39	470	0.46	470	0.58
Calculation	Ca	2.84	Ca	2.53	Ca	3.10
	Cb	0.45	Cb	0.80	Cb	1.03
	Ca+b	3.28	Ca+b	3.33	Ca+b	4.13
Carotenoids (µg/mL extract)	Cx+c	1.75	Cx+c	1.95	Cx+c	2.48

Table D.3 Summary: Carotenoids Production under Stress. in Macro Tests (Flasks), Microalgae: *Dunaliella salina* (µg/mL extract and pg/cell)

Salinity (ppt)	120	170	220
Day 0 (µg/mL extract)	0.74	0.75	0.79
Day 7 (µg/mL extract)	1.75	1.95	2.48
Production (µg/mL extract)	1.01	1.21	1.69
Day 0 (pg/cell)	2.43	2.46	2.61
Day 7 (pg/cell)	0.78	1.74	3.58
Production (pg/cell)	-1.65	-0.72	0.97

APPENDIX E: MICROALGAE RETENTION MESH .

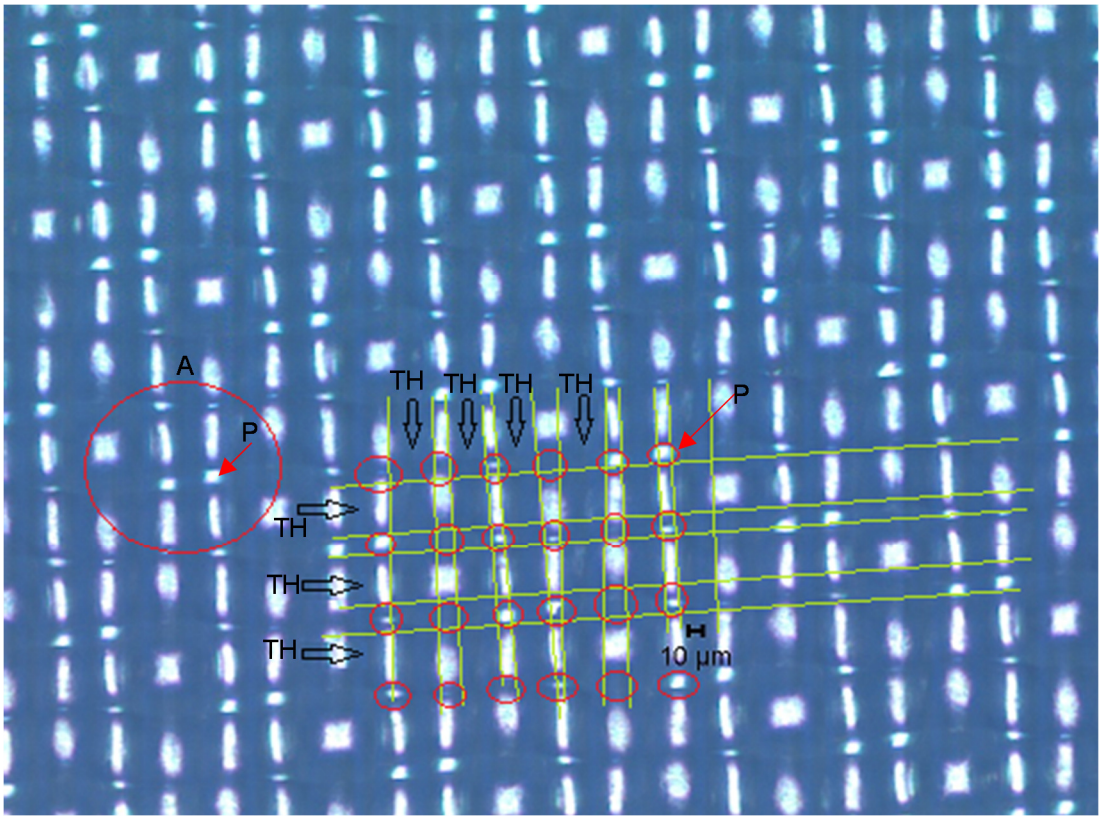

Figure E.1 Cell retention mesh microscope view. Different pores defined by Nylon single threads crossing configuration. Threads delimited in the picture by green lines forming a matrix. The matrix is made up of a first layer of parallel threads on top of a second layer of parallel threads at 90 degrees, one respect the other. (A) Pore area showing different pore sizes respect to other areas; pore (each small red circle delimit a pore) (P); Nylon thread and direction (TH).

APPENDIX F: VIEWS OF MICROALGAE INSIDE MICROCHAMBER AND RETAINING MESH AT THE TOP OF IT.

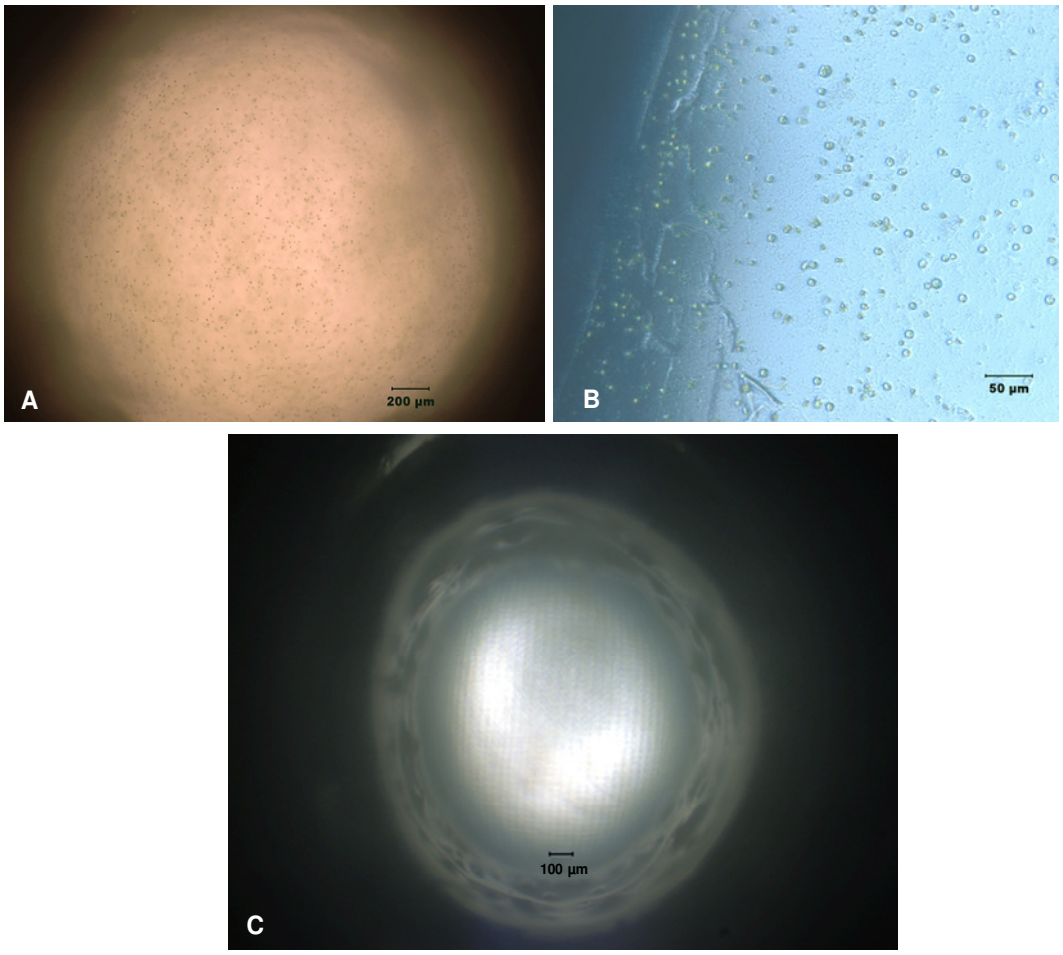

Figure F.1 Views of Microalgae inside Microchamber and Retaining Mesh. (A) Cells floating inside microchamber; (B) Cells at the bottom of microchamber, touching glass slide and not being able to be removed or agitated by incoming media flow; (C) upper area view of microchamber taken from bottom window, before reaching the micromesh for algae retention (micromesh Nylon fibers can be noticed).

APPENDIX G: SIGNAL COMING FROM PHOTODETECTOR SENSOR.

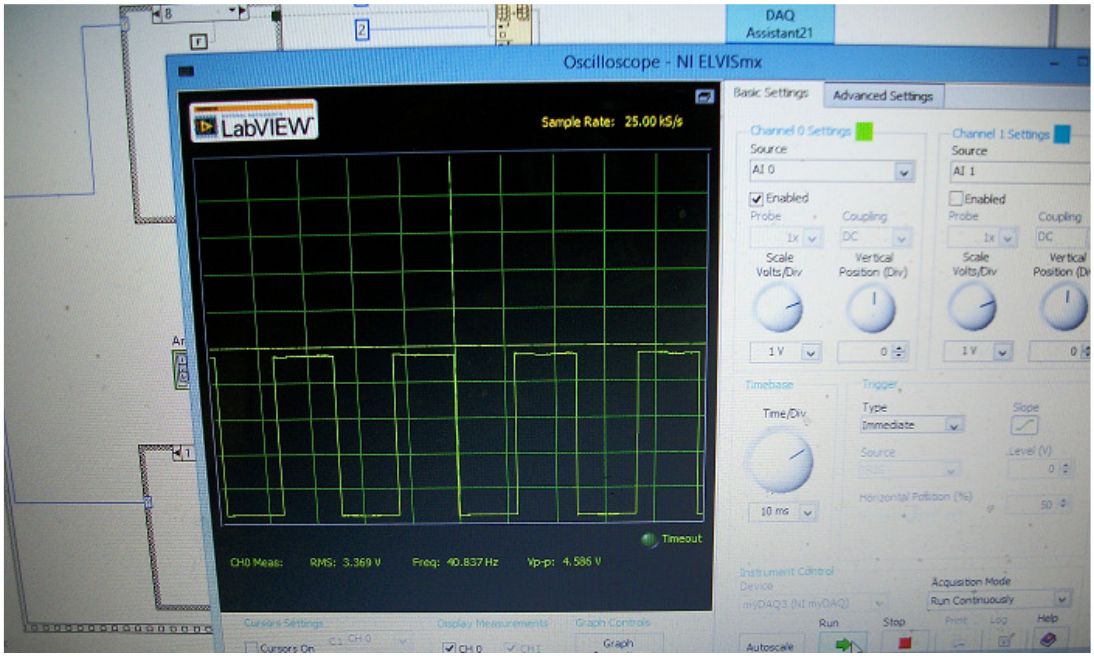

Figure G.1 Measuring signal frequency coming from photodetector array. Scattered green light detected at 90 degrees due to different turbidity levels, related to microalgae density inside the microchamber. In this case frequency is directly proportional to increases in light irradiance.

APPENDIX H: CO_2 SOLUBILITY IN SEA WATER

Table H.1 CO_2 SOLUBILITY IN SEA WATER (Al-Anezi et al [49])

Solubility data of the gases dissolved in seawater with S = 35 g/kg in equilibrium with the atmosphere at 25°C

Gas	Partial pressure in atmosphere [bar]	Henry's law coefficient [mol/(m^3 bar)]	Concentration in seawater [μmol/kg SW]	Concentration in seawater [mg/kg SW]
Co_2	0.00033	29.3	9.45	0.4
N_2	0.7808	0.5	383.4	10.7
O_2	0.2095	1.0	206.3	6.6
Ar	0.00934	1.1	10.11	0.4

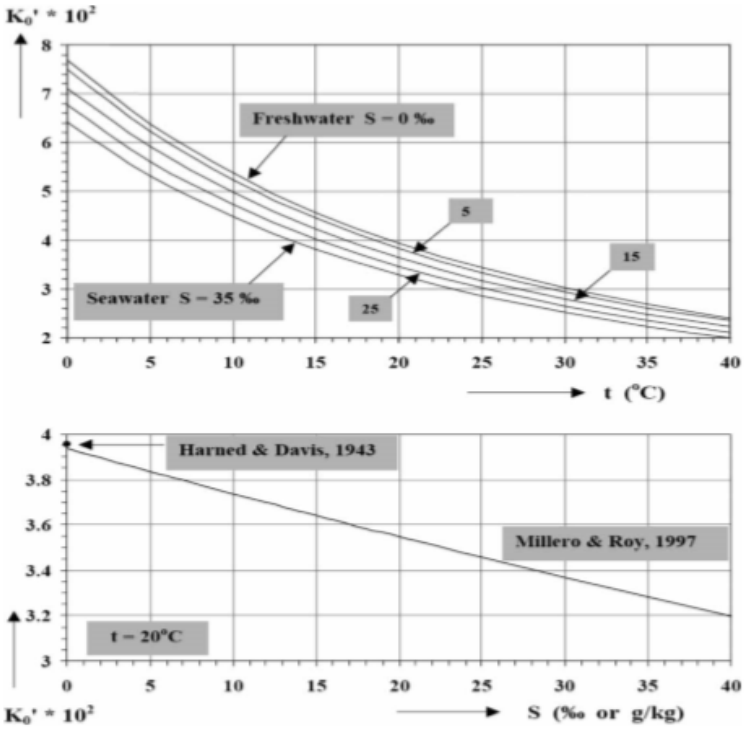

The solubility constants (=solubilities in M/L.atm) for CO_2 in freshwater, seawater and brackish water as a function of temperature at salinities of 0, 5, 15, 25, and 35‰ (=g of salt per kg of water) (upper graph) and as a function of salinity at 20°C (lower graph).

Figure H.1 CO_2 solubility in sea water. (Al-Anezi et al [49])

BIOGRAPHY OF THE AUTHOR

Cristián Andrés Cox Seguel was born in Rancagua, Chile in 1970. He obtained an Industrial Electronics technical degree in 1991 from INACAP, Chile. In 1988 he graduated from Universidad Nacional Andrés Bello, Chile, with a Bachellor of Science in Aquaculture Engineering. In 2011 he enrolled in the Biological Engineering graduate program at University of Maine, Orono.

He has worked for several companies and entities related to biotechnology, biomedical devices and instruments, aquaculture automation, machinery and water recirculation systems for aquaculture. Nowadays he works for a new aquaculture proyect at Atacama desert, Chile. Cristián Cox is a candidate for the Master of Science degree in Biological Engineering at The University of Maine in December, 2016.